

Direction of Arrival Estimation Using Maximum Likelihood Method  
and the Effect of Element Selection on System Performance

Mohammad Hazem Moussa

A Thesis  
in  
The Department  
of  
Electrical and Computer Engineering

Presented in Partial Fulfillment of the Requirements  
for the Degree of Master of Applied Science (Electrical Engineering) at  
Concordia University  
Montreal, Quebec, Canada

August 2005

© Mohammad Hazem Moussa, 2005



Library and  
Archives Canada

Bibliothèque et  
Archives Canada

Published Heritage  
Branch

Direction du  
Patrimoine de l'édition

395 Wellington Street  
Ottawa ON K1A 0N4  
Canada

395, rue Wellington  
Ottawa ON K1A 0N4  
Canada

*Your file* *Votre référence*

*ISBN: 0-494-10244-6*

*Our file* *Notre référence*

*ISBN: 0-494-10244-6*

#### NOTICE:

The author has granted a non-exclusive license allowing Library and Archives Canada to reproduce, publish, archive, preserve, conserve, communicate to the public by telecommunication or on the Internet, loan, distribute and sell theses worldwide, for commercial or non-commercial purposes, in microform, paper, electronic and/or any other formats.

The author retains copyright ownership and moral rights in this thesis. Neither the thesis nor substantial extracts from it may be printed or otherwise reproduced without the author's permission.

#### AVIS:

L'auteur a accordé une licence non exclusive permettant à la Bibliothèque et Archives Canada de reproduire, publier, archiver, sauvegarder, conserver, transmettre au public par télécommunication ou par l'Internet, prêter, distribuer et vendre des thèses partout dans le monde, à des fins commerciales ou autres, sur support microforme, papier, électronique et/ou autres formats.

L'auteur conserve la propriété du droit d'auteur et des droits moraux qui protègent cette thèse. Ni la thèse ni des extraits substantiels de celle-ci ne doivent être imprimés ou autrement reproduits sans son autorisation.

---

In compliance with the Canadian Privacy Act some supporting forms may have been removed from this thesis.

Conformément à la loi canadienne sur la protection de la vie privée, quelques formulaires secondaires ont été enlevés de cette thèse.

While these forms may be included in the document page count, their removal does not represent any loss of content from the thesis.

Bien que ces formulaires aient inclus dans la pagination, il n'y aura aucun contenu manquant.

  
**Canada**

## Abstract

This thesis was performed by first understanding the concept of DoA estimation and realizing its importance and applications. Second, DoA estimation techniques, which are not few and vary in principle and applications, were reviewed in order to find the most suitable technique to use in this thesis. The target is to find a DoA technique that is simple to construct to illustrate the effect of mutual coupling and array antenna element selection on the DoA estimation process, and at the same time, to be a technique from which the obtained results could be generalized to more specific cases rather than one or two cases. The Maximum Likelihood Method was found to be the most suitable DoA technique. Third, the MLM was implemented using both, omni-directional elements and point sources as the array antenna elements. Fourth, NEC2 was introduced, its theoretical and principal of operation were explained. Also mutual coupling between the array elements was introduced as it affects the over all performance of the array structure in DoA estimation. Finally, a NEC2-Matlab interface was implemented to produce Mean Square Error graphs for different scenarios using the MLM and  $\lambda/2$  dipole antennas as the array elements and then  $\lambda/2$  dipole antennas above perfectly conducting ground plane. This change of elements in the array structure produced a significant enhancement in the DoA performance. Another approach that was also tested was changing the spacing between the array elements. This approach, under certain conditions, also showed a significant enhancement in the DoA estimation performance.

## **Acknowledgments**

First of all, I would like to express my unlimited gratitude to God for all what I achieved. My special thanks go to Dr. Sebak for all his support, patience, and for understanding the special circumstances I had to work under. He was a great and an inspiring professor to be involved in research with.

I would also like to thank my family for all their support and their help in taking the right decision in the right time. If my thanks could reach my father right now, then I would like to tell him thank you very much for your support, thank you for raising me to be the person I am right now, thank you for believing in me, thank you for teaching me so many things that I would have never learned without you. Rest in peace and God bless your soul.

I am very grateful to all my friends especially Mohammad Abou-Khousa for being very helpful and supportive through the good and the bad times.

## **Dedication**

To my father, God bless his soul, my mother, and my sister.

# Table of Contents

List of Figures.....	viii
List of Symbols.....	xi
Chapter 1: Introduction.....	1
1.1    Motivations.....	1
1.2    Objectives.....	2
1.3    Overview of the Document.....	2
Chapter 2: Literature Review.....	4
2.1    Array Theory Background.....	4
2.2    Direction of Arrival (DoA) Estimation Methods.....	8
2.3    Numerical Electromagnetic Code NEC2.....	15
Chapter 3: Maximum Likelihood Method.....	18
3.1    Theoretical Background.....	19
3.2    Statistical Analysis for Determining MSE.....	25
Chapter 4: NEC, Method of Moments, and Mutual Coupling.....	35
4.1    Method of Moments.....	36
4.1.1    Pocklington's Integral Equation.....	37
4.1.2    Hallen's Integral Equation.....	38
4.1.3    Method of Moments Solution.....	39
4.2    Method of Moments and Wire Array Antennas.....	41
4.3    Wire Modeling Using NEC2.....	42
4.4    Mutual Coupling.....	43
4.5    Summary and Illustrative Experiment.....	52
Chapter 5: Development of NEC2-Matlab Interface.....	55
5.1    NEC2 Input/Output Files Format.....	55

5.2	NEC2-Matlab Interface.....	56
5.2.1	NEC2-Matlab Interface Commands and Procedure.....	56
Chapter 6: NEC2/MLM Simulation Results and Element Selection.....		61
6.1	Input Impedance of a $\lambda/2$ Dipole Antenna.....	61
6.2	$\lambda/2$ Dipoles and $\lambda/2$ Dipoles Above Perfectly Conducting Ground Plane.....	65
6.2.1	Approximation of a Micro-strip Patch.....	65
6.2.2	Maximum Directivity $D_o$ .....	67
6.3	Simulations Results.....	70
4.4	Summary.....	78
Chapter 7: Conclusion.....		80
7.1	Summary.....	80
7.2	Concluding Remarks.....	82
7.3	Future Work.....	83
References.....		85

## List of Figures

<b>Figure 2.1:</b> Linear and planner arrays.....	4
<b>Figure 2.2:</b> An incident plane wave arriving at a linear array at an angle of $\theta_o$ from normal to the array.....	6
<b>Figure 3.1:</b> 3-element and 5-element $\lambda/2$ dipole linear arrays geometry.....	24
<b>Figure 3.2:</b> Three trial run for the 3-element linear array.....	27
<b>Figure 3.3:</b> Three trial run for the 5-element linear array.....	28
<b>Figure 3.4:</b> Comparison, in terms of MSE, between a 3-element linear array and a 5-element linear array.....	29
<b>Figure 3.5:</b> Comparison, in terms of MSE, between a 3-element linear array with and without element pattern (dipole) included.....	30
<b>Figure 3.6:</b> Comparison, in terms of MSE, between a 5-element linear array with and without element pattern (dipole) included.....	31
<b>Figure 3.7:</b> Changing the spacing between the elements for a 3-element linear array.....	32
<b>Figure 3.8:</b> Changing the spacing between the elements for a 5-element linear array.....	33
<b>Figure 4.1:</b> Uniform plane wave obliquely incident on conducting wire.....	37
<b>Figure 4.2:</b> Illustration of the effect of mutual coupling.....	45
<b>Figure 4.3:</b> Real part of input impedance as a function of the operating frequency for a single dipole, center element and edge element of a 5-element linear array.....	47
<b>Figure 4.4:</b> Imaginary part of input impedance as a function of the operating frequency for a single dipole, center element and edge element of a 5-element linear array.....	48



<b>Figure 4.5:</b> Real part of input impedance as a function of the operating frequency for a single dipole, center element and edge element of a 5-element linear array with 0.6 lambda inter-element spacing.....	49
<b>Figure 4.6:</b> Imaginary part of input impedance as a function of the operating frequency for a single dipole, center element and edge element of a 5-element linear array with 0.6 lambda inter-element spacing.....	50
<b>Figure 4.7:</b> Radiation pattern of a 5-element linear $\lambda/2$ dipole array antenna with and without mutual coupling.....	51
<b>Figure 4.8:</b> MSE for the MLM with no mutual coupling.....	53
<b>Figure 4.9:</b> Comparison between the "without mutual coupling" case and the "with mutual coupling" case.....	53
<b>Figure 6.1:</b> Input resistance of a center-fed $\lambda/2$ dipole antenna as a function of its length.....	63
<b>Figure 6.2:</b> Input reactance of a center-fed $\lambda/2$ dipole antenna as a function of its length.....	64
<b>Figure 6.3:</b> Radiation pattern at $\Phi = 0^\circ$ .....	68
<b>Figure 6.4:</b> Radiation pattern at $\Phi = 90^\circ$ .....	69
<b>Figure 6.5:</b> Radiation pattern at $\Phi = 90^\circ$ .....	70
<b>Figure 6.6:</b> Comparison in terms of MSE between a 5-element dipole linear array in free space and a 5-element dipole linear array above perfectly conducting ground plane.....	71
<b>Figure 6.7:</b> Comparison in terms of MSE between a 5-element dipole linear array in free space and a 5-element dipole linear array above perfectly conducting ground plane.....	72

**Figure 6.8:** Comparison in terms of MSE between a 5-element dipole linear array in free space with 0.5 Lambda and 0.6 lambda spacing between the elements.....74

**Figure 6.9:** Comparison in terms of MSE between a 5-element dipole linear array above perfectly conducting ground plane with 0.5 Lambda and 0.6 lambda spacing between the elements.....75

## List of Symbols

$\theta$ :	Angle measured from the z-axis.
$\phi$ :	Angle measured from the x-axis.
$\lambda$ :	Wavelength in meters.
$\theta_o$ :	Angle of arrival of an incident plane wave on a linear array.
$\phi_o$ :	Electric Angle of Arrival.
$k$ :	Wave number.
$d$ :	Interelement spacing of a linear equispaced array.
$\omega$ :	Angular frequency.
$F_s$ :	Sampling frequency.
$M, m$ :	Number of array antenna elements.
$n$ :	Number of signals incident on the array antenna.
$e(t)$ :	Complex Additive White Gaussian Noise.
$A^T$ :	Transpose of $A$ .
$A^*$ :	Conjugate transpose of $A$ .
$E$ :	The expectation operator.
$\sigma^2$ :	Noise variance.
$\hat{A}$ :	ML estimate of $A$ .
$\hat{\theta}$ :	ML estimate of $\theta$ .
$\hat{x}(t)$ :	ML estimate of $x(t)$ .
$MSE$ :	Mean Square Error.
$ML$ :	Maximum Likelihood.
$S$ :	Standard deviation.
$DoA$ :	Direction of Arrival.

$I_z(z')$ :	The equivalent filamentary line-source current located on the surface of the wire.
$a, \rho, a$ :	Radius of the wire.
$R$ :	Distance from the wire segment under consideration to the observation point.
$E_z^i$ :	Tangential component of the electric field incident on the wire.
$\Delta$ :	Segment length.
$SNR$ :	Signal to Noise ratio.
$\epsilon_e$ :	Effective dielectric constant of the micro-strip line.
$\epsilon_r$ :	Relative dielectric constant of the material.
$h$ :	The thickness of the dielectric material in a micro-strip patch.
$h'$ :	The distance between the dipole antenna and the ground plane.
$W$ :	The width of the micro-strip line.
$\lambda_e$ :	Wavelength in the dielectric material.
$D_o$ :	Maximum directivity.
$\Theta_{r1}, \Theta_{r2}$ :	Half power beam width in two perpendicular planes, in radians.
$R_r$ :	Radiation resistance.

# Chapter 1

## Introduction

### *1.1 Motivations*

The problem of determining the direction of arrival (DoA) of narrow band plane waves incident on passive sensor antennas have been of great importance and received significant attention in the recent signal processing research. The latest research trends moved towards utilizing array antennas, either linear or planar, in order to determine the DoA of plane waves incident on them. This approach has a wide range of applications that varies from radar systems—i.e. jamming and target locating, to wireless communications. For instance, in a radar system, DoA estimation is of great importance in order to locate the signal arriving from a potential target. Electronic steering in this case would replace mechanical steering of the radar antenna. Also, in a wireless communication environment, determining the DoA of the desired user signal at the base station would result in minimizing the interference from other users. This may be done by either directing the main beam of an array antenna towards the desired user or by directing nulls towards the interfering users.

Several direction of arrival estimation techniques exist in the literature [1]-[5], and they have been widely and deeply studied since the 1980's. Most of these studies were focused on the signal processing side of the DoA technique and ignored the array side or in other words, assumed either omni-directional elements or isotropic elements in the array structure. They also ignored the existence of mutual coupling between the array elements. From an antenna design point of view, these factors play

a major role in the performance of a DoA estimation system. Therefore, a study that investigates the effect of using more directive elements in the array structure and accounts for mutual coupling between the array elements for direction of arrival estimation would be of great importance in order to assess how such a DoA estimation system would perform in more realistic conditions. To achieve this goal, first, a DoA estimation technique should be selected from the techniques available in the literature and second, integrating Matlab and Numerical Electromagnetic Code NEC2. This integration gives the ability to account for mutual coupling between the array elements and to come up with a fully integrated system that is controlled completely by Matlab. It also gives the flexibility to change the elements in the array structure. The focus of this thesis is directed towards the analysis of the DoA estimation performance and how to enhance it.

## ***1.2 Objectives***

The objective of this thesis is to integrate Matlab and Numerical Electromagnetic Code NEC2 in conjunction with a DoA estimation method to form a DoA estimation system. Further more, the objective includes a study of the effect of mutual coupling between the array elements and the effect of changing the array elements type on the direction of arrival estimation process.

## ***1.3 Overview of the Document***

This thesis is divided into the following chapters in order to explain the work done and the results obtained. Chapter 2 presents a review of the array theory, the existing DoA estimation methods, and Numerical Electromagnetic Code NEC2.

Chapter 3 is about the Maximum Likelihood Method. It includes the theory behind this method, an implementation of the MLM for 3-element and 5-element  $\lambda/2$  dipole linear arrays, statistical analysis for the confidence interval of the results obtained by the MLM, and simulation results for different cases.

Chapter 4 is about NEC2, Method of Moments, and Mutual Coupling. It introduces NEC2 and its theoretical background. It provides a discussion about the Method of Moments used in NEC2 to solve the integral equations. It also explains the principal of wire modeling in NEC2. Since NEC2 accounts for mutual coupling effects between the array elements, a brief review of the mutual coupling principal is introduced and two experiments were conducted to illustrate the effect of mutual coupling on an array in the transmit and receive modes.

Chapter 5 fully explains the integration process between NEC2 and Matlab. NEC2-Matlab interface is a very important section of this chapter. It explains how both softwares are integrated. It includes the commands used by Matlab and some modifications done on NEC2 source code to make it more suitable for the integration.

Chapter 6 presents a set of results obtained from running the NEC2-Matlab integrated system. It provides a comparison for different cases and it includes the effect of element selection on the DoA estimation process. It also shows the effect of changing inter-element spacing, under certain conditions, on the DoA estimation process.

Chapter 7 is the last chapter of this thesis and it includes a summary of the work done, concluding remarks, and some suggestions for future work.

# Chapter 2

## Literature Review

### 2.1 *Array Theory Background*

Array antennas vary considerably in shape and element type. Different array geometry, such as linear, circular, rectangular, and spherical arrays, and elements types are currently being investigated for their potential advantages in many fields, such as wireless communications.

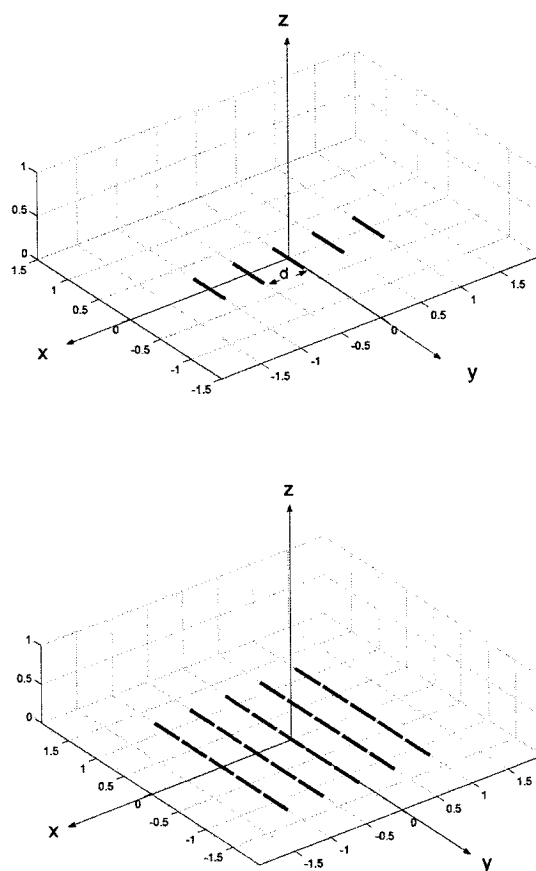


**Figure 2.1:** Linear and planar arrays [6]



Figure 2.1 shows a linear and a planar array of antenna elements. The antenna elements lie in the  $xy$  plane, with the  $z$ -axis perpendicular to the array and pointing in the broadside direction. An antenna element can be any physical antenna, such as a monopole antenna, dipole antenna, or micro-strip patch.

In this thesis, the excitation of the array is assumed to be a plane wave, and its direction is measured with respect to the  $z$ -axis using the standard spherical polar coordinates  $\theta$ , measured from the  $z$ -axis and  $\phi$ , measured from the  $x$ -axis. This thesis deals only with the case of a linear array, but the principal is applicable to planar arrays as well.

Three important points should be taken into consideration when array antennas are being investigated:

1. Array factor
2. Element pattern
3. Mutual coupling between the array elements.

Each array has its own array factor. The array factor, in general, is a function of the number of elements, their geometrical arrangement, their relative magnitudes, their relative phases, and their spacing. In general, elements are spaced apart a distance of half-wavelength ( $\lambda/2$ ) of the operating frequency. Inter-element spacing larger than  $\lambda/2$  gives rise to grating lobes. Grating lobes are a periodic repetition of the primary pattern due to the spacing, in which more than one main lobe would start to appear in the overall radiation pattern of the array.

The element pattern plays an important role in reducing the mutual coupling effects between the array elements. Therefore, different element selection criteria should be adopted for different applications. Mutual coupling is the process of energy

transfer and re-scattering of the energy between the array elements. It is discussed in more details in chapter 4, section 4.4.

Given a linear array of elements, with an incident plane wave arriving at  $\theta_o$ , the signal received at each element will differ in phase based upon the propagation constant,  $k$ , and the element spacing,  $d$ . From figure 2.2, the delay distance is  $d \sin\theta_o$ , which, when combined with the propagation constant,  $k = \frac{2\pi}{\lambda}$  produces a progressive phase delay of  $\phi_o = kd \sin\theta_o$ , between the elements. The inter-element phase delay, given by:

$$\phi_o = kd \sin\theta \tag{2.1}$$

And it is known as electrical angle of arrival.

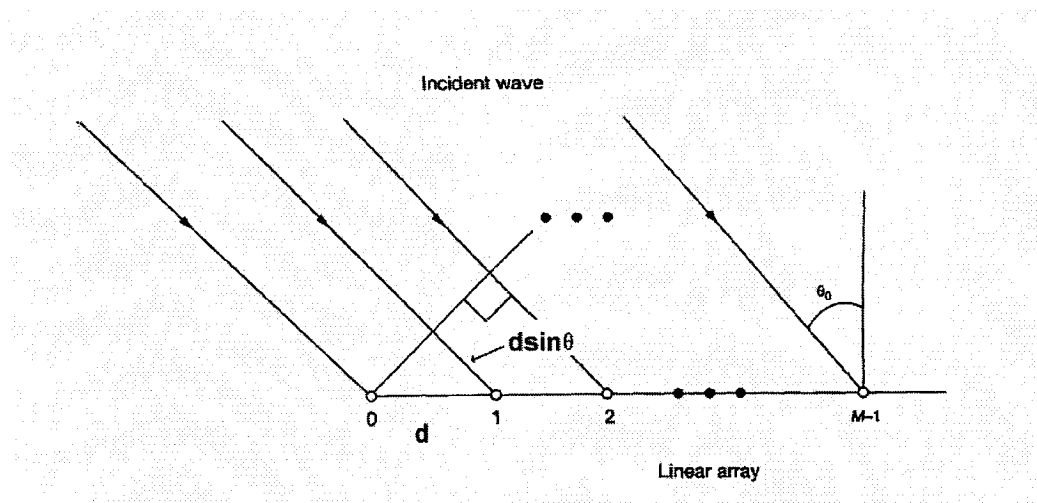


**Figure 2.2:** An incident plane wave arriving at a linear array at an angle of  $\theta_o$  from normal to the array [6]

Consider the linear array antenna of  $M$  elements shown in figure 2.2. The array is illuminated by an incident plane wave, which when sampled is of the form:

$$u(n) = e^{j(\omega_u n - k\bar{r})} \quad (2.2)$$

where  $\omega = 2\pi f$  is the angular frequency,  $k$  is the wave number, and  $n$  would take on uniformly spaced instances in time given the sampling frequency,  $F_s$ .

For a linear array of elements, with an incident plane wave arriving at  $\theta_o$ , the signal received at each element will differ in phase based upon the propagation constant,  $k$ , and the element spacing,  $d$ , as shown in figure 2.2. Given the separation distance of  $d$  meters, the path length difference is  $d \sin\theta_o$  meters. At any given instant in time, a line perpendicular to the direction of arrival of the plane wave is, by definition, a line of constant phase. For a propagation constant, or wave number, of  $k = \frac{2\pi}{\lambda}$  radians per meter, this translates into a phase delay of  $\phi_o = kd \sin\theta_o$  between each element.

If an end element is designated as the first, or  $0^{\text{th}}$ , element, the phase progression across the array is given by:

$$s(\phi) = [1, e^{-j\phi}, \dots, e^{-j(M-1)\phi}]^T \quad (2.3)$$

where  $T$  is the transpose operator, and  $M$  is the number of antenna elements. This vector,  $s(\phi)$ , is called the steering vector because it steers the direction of the main beam of the array. That is, by multiplying the vector of signals received at the antenna terminals by the steering vector, the inner product is the delayed and summed output of the array.

The output of the array,  $y(n)$ , is given by:

$$y(n) = u_0(n) \sum_{k=0}^{M-1} w_k^* e^{-jk\phi_0} \quad (2.4)$$

where  $u_0(n)$  is the signal received at time  $n$  by the end antenna element, 0<sup>th</sup> element, in figure 2.2. The  $w_k^*$  in (2.4) represent the driving-point voltage or current for a transmit mode, or the scaling factor (weighting) of the electrical signals (current or voltage) at the antenna terminals in receive mode.

The normalized array factor for a uniform weighting is given by:

$$AF = \frac{1}{M} \sum_{k=0}^{M-1} e^{-jk(\phi_0 - \phi)} = w_q^H s(\phi) \quad (2.5)$$

where  $H$  is the Hermitian operator of conjugate transpose,  $\phi_0$  is the electrical scan angle and  $\phi$  is the electrical angle of the point in space where the array factor is to be calculated. To produce a normalized directive gain radiation pattern for a given array scanned to an electrical angle  $\phi_0$  across field of view given by  $-90^\circ \leq \theta \leq 90^\circ$ , one need only choose a suitable number of  $\theta$  angles as far-field sample points, convert them to the electrical angle using (2.3), and perform the summation given in (2.5), or perform the vector inner product of the weights with the steering vector [6].

## 2.2 *Direction of Arrival (DoA) Estimation Methods*

Array antennas have been of great importance in Direction of Arrival estimating algorithms since they have the ability to extract information about the incident signal that other types of antennas would fail to extract. Due to the fact that a

simple linear array consists of multiple elements (sensors), the incident plane wave could be sampled at various locations. The samples consist of amplitude and phase information needed to determine the direction of arrival of a signal.

This section provides a brief review of the DoA estimation methods and full details about their performance, sensitivity, and limitations could be found in [5] and the references therein.

Based on this review, a DoA estimation technique is going to be adopted for future analysis in this thesis.

### *2.2.1 Spectral Estimation Methods*

The principal in these methods for DoA estimation is computing the spatial spectrum and then determining the local maximas. One of the earliest methods of this type is the Bartlett method. The method is based on creating a list of steering vectors for the array, estimating the mean power coming from different directions, and finding the corresponding steering vector associated with the direction  $\theta$ . This process is similar to steering the array mechanically in the direction of the maximum power [7], [8], [9].

### *2.2.2 MVDR Estimator*

The Minimum Variance Distortionless Response estimator is a Maximum Likelihood method of spectrum estimation. This method uses array weights, which are obtained by minimizing the mean output power subject to unity constraints in the look direction [5]. This method outperforms Bartlett method in terms of resolution properties but it does not possess the optimum resolution properties [7], [10].

### 2.2.3 *Linear Prediction Method*

This method estimates the output of one sensor using linear combinations of the remaining sensor outputs and minimizes the mean square prediction error. This method performs well in a moderately low SNR environment, and when the sources are of approximately equal strength and are nearly coherent [8], [11].

### 2.2.4 *MEM*

The Maximum Entropy Method finds a power spectrum such that its Fourier transform equals the measured correlation subjected to the constraint that its entropy is maximized. When applied to DoA estimation using an array of sensors, this method finds a continuous power function than maximizes the entropy function subject to certain constraints [12], [13].

### 2.2.5 *MLM*

The Maximum Likelihood Method estimates the DoA from a given set of array samples by maximizing the log-likelihood function. The likelihood function is the joint probability density function of the sampled data given the DoA's and viewed as a function of the desired variables which are the DoA's in this case. The operation principal of this method is to search for the directions that maximize the log of the likelihood function. The ML criterion signifies that plane waves from these directions are most likely to cause the given samples to occur. The MLM gives a superior performance compared to other methods, especially, at low SNR, number of samples is small or the sources are correlated [1], [5], [10].

### 2.2.6 *Eigenstructure Methods*

Eigenstructure-based methods search for directions such that the steering vectors associated with these directions are orthogonal to the noise subspace and are contained in the signal subspace. This search may be divided in two parts. Part one, find a weight vector that is contained in the noise subspace or is orthogonal to the signal subspace. Part two, search for directions such that the steering vectors associated with these directions are orthogonal to this vector.

These methods depend on some properties of the array correlation matrix  $R$ .

These properties include:

1. The space spanned by its eigenvalues may be partitioned into two subspaces, which are the signal subspace and the noise subspace.
2. The steering vectors corresponding to the directional sources are orthogonal to the noise subspace. Since the noise subspace is orthogonal to the signal subspace, the steering vectors are contained in the signal subspace.

An important point to mention is that the noise subspace is spanned by the eigenvectors associated with the smaller eigenvalues of the correlation matrix, and the signal subspace is spanned by the eigenvectors associated with the larger eigenvalues of the correlation matrix.

There exist many methods that are based on eigenstructure, some of them are going to be discussed briefly in this part of the introduction. Further details could be found in [5] and the reference therein.

### 2.2.7 MUSIC Algorithm

The Multiple Signal Classification (MUSIC) algorithm is a relatively simple and efficient eigenstructure method for DoA estimation. It takes different forms and they are the following:

#### 1. Spectral MUSIC

This is known as the standard form of the MUSIC method. It estimates the noise subspace from the available samples. This can be done by either eigenvalue decomposition of the estimated array correlation matrix or singular value decomposition of the data matrix, with its  $N$  columns being the  $N$  snapshots or the array signal vectors. After estimating the noise subspace, this method searches for  $M$  directions by looking for steering vectors that are as orthogonal as possible to the estimated noise subspace. Another alternative is to use the signal subspace and search for directions with steering vectors contained in this space.

For a single source, MUSIC method was able to asymptotically approach the CRLB. Cramer-Rao Lower Bound (CRLB) is the theoretically lowest value of the covariance of an unbiased estimator. However, MUSIC approaches CRLB only when the number of snapshots increases infinitely. For multiple sources, the same hold but the condition to approach CRLB is that SNR approaches infinity [14], [15].

#### 2. Root-MUSIC

In this algorithm, for a uniformly spaced linear array, the DoA search is made by finding the roots of a polynomial. It solves a polynomial rooting problem compared to the identification and localization of spectral peaks using Spectral MUSIC. Root-MUSIC has a better performance than Spectral MUSIC [5].



### 3. Constrained MUSIC

This method utilizes the knowledge of the known source to improve the estimates of the unknown source direction. It is only applicable when some of the source directions are already known. This method removes the components of the signal induced by these known sources from the data matrix and then uses the modified data matrix for DoA estimation [15].

### 4. Beam-Space MUSIC

The MUSIC algorithms described above may be thought of as element-space algorithms since they are based on processing the snapshots received from the sensor elements without any preprocessing, such as beam formation. In Beam-Space MUSIC algorithm, the array data are passed through a beam-forming processor before applying MUSIC or any other DoA estimation algorithm. The output of the beam-forming processor may be thought of as a set of beams; therefore, processing using this data is referred to as beam-space processing. This method has a number of advantages such as reduced computations, improved resolution, reduced sensitivity to system errors, reduced resolution threshold, reduced bias in the estimate, etc. The reason behind these advantages is that the number of beams formed by the beam former is less than the number of array elements. A limitation that arises in this method comes from the fact that element-space methods have degrees of freedom equal to the number of elements in the array, whereas, in beam-space methods, the degrees of freedom are equal to the number of beams formed by the beam-forming filter. Hence, this process reduces the degrees of freedom of the array [16], [17].

### 2.2.8 *Min-Norm Method*

This method is applicable to uniformly spaced linear arrays and it finds the DoA estimate by searching for the location of peaks in the power spectrum. The optimization problem of this method to find the array weights, and therefore DoA, could be transformed to a polynomial rooting problem, leading to a root-min-norm method similar to the root-MUSIC method. The performance of both methods has been compared and the comparison indicated that the variance in the estimate obtained by root-MUSIC is smaller than or equal to that of the root-min-norm method [18], [19].

### 2.2.9 *CLOSEST Method*

The name CLOSEST comes from the fact that this method searches for array weights in the noise subspace that are close to the steering vectors corresponding to the DoA's in the sector under consideration. Contrary to beam-space methods, which work by first forming beams in selected directions, this method operates in the element space and could be thought of as an alternative to beam-space MUSIC [20].

### 2.2.10 *ESPRIT*

Estimation of Signal Parameters via Rotational Invariance Techniques (ESPRIT) is a computationally efficient and robust method in DoA estimation. It uses two identical arrays in the sense that array elements need to form matched pairs with an identical displacement vector. This doesn't mean that one has to have two separate arrays. But this could be achieved by changing the array geometry in a way that the elements could have this property [21].

### 2.2.11 *WSF Method*

The Weighted Subspace Fitting (WSF) is a unified approach to schemes like MLM, MUSIC, and ESPRIT. It requires knowledge of the number of directional sources. The method finds the DoA such that the weighted version of a matrix whose columns are the steering vectors associated with these directions is close to a data-independent matrix. The data-independent matrix could be a Hermitian square root of the array correlation matrix or a matrix whose columns are the eigenvectors associated with the largest eigenvalues of the array correlation matrix [5], [22], [23].

## 2.3 *Numerical Electromagnetic Code NEC2*

A major part of this thesis is based on integrating NEC2 with Matlab. The Numerical Electromagnetic Code (NEC2) is a user-oriented program developed at Lawrence Livermore Laboratory [24]. It is a method of moments' code for analyzing the interaction of electromagnetic waves with arbitrary structures consisting of conducting wires and surfaces. It combines an integral equation for smooth surfaces with one for wires to provide convenient and accurate modeling for a wide range of applications. The code can model non-radiating networks and transmission lines, perfect and imperfect conductors, lumped element loading, and perfect and imperfect conducting ground planes. It uses the electric field integral equation (EFIE) for thin wires and the magnetic field integral equation (MFIE) for surfaces. The excitation can be either an applied voltage source or an incident plane wave arriving from predefined angle or set of angles. The program computes induced currents and charges, near- and far-zone electric and magnetic fields, radar cross section, impedances or admittances, gain and directivity, power budget, and antenna-to-antenna coupling [25]. There are

several commercial NEC2 packages available, built on the freely available source code, and offering a graphical user interface (GUI) and post-processing visualization tools. There is Mini-NEC from EM Scientific Corp., the NEC-Win series from Nittany Scientific, Inc. and the popular SuperNEC from The Poynting Group. The prices range from a few hundred to a few thousand dollars, with some limited version free downloads available [6].

On the other hand, Matlab is a high-level technical computing language and interactive environment for algorithm development, data visualization, data analysis, and numerical computations. Using Matlab, one can solve technical computing problems faster than with traditional programming languages, such as C, C++, and FORTRAN.

Matlab can be used in a wide range of applications such as signal and image processing, communications, control design, test and measurement, financial modeling and analysis, and computational biology. Add-on toolboxes (collections of special-purpose Matlab functions) extend the Matlab environment to solve particular classes of problems in these application areas.

One of the most important features of Matlab is that it is possible to integrate a Matlab code with other languages and applications, and distribute the Matlab algorithms and applications. This feature is going to be of particular interest in this thesis. It contains functions for integrating Matlab based algorithms with external applications and languages, such as C, C++, FORTRAN, Java, COM, and Microsoft Excel. It also possesses an advanced file I/O and graphical display capabilities such as two dimensional and three dimensional graphs [26].

This work demonstrates the integration of NEC2 with Matlab. NEC2 is used for the electromagnetic computations and Matlab is used for creating input files for

NEC2, reading the output files of NEC2, performing the signal processing part of the simulations, and graphically displaying the results. NEC2 input files follow very strict rules in terms of command line order and spacing. The numerical data can be prepared in Matlab and then put in NEC2 input file format with the appropriate strings and written to a text file. Matlab can call the NEC2 executable from within one of its scripts (called m-files), and then read in the resulting NEC2 output file for further analysis and processing. Therefore, NEC2 becomes a tool driven by Matlab. By performing this integration step, Matlab could take control of any iterative procedure in order to obtain the needed results.

## Chapter 3

### Maximum Likelihood Method: Review

The Maximum Likelihood Method (MLM) is adopted in determining DoA after information about the incident wave has been extracted from the array elements. In addition, integration between Matlab and NEC2 is proposed in this thesis to construct a complete DoA estimation system that utilizes the MLM as the DoA estimation algorithm.

The Maximum Likelihood Method (MLM) has been widely studied in the literature [1]-[4]. The MLM estimates the DoA from a given set of array samples by maximizing the log-likelihood function. The likelihood function is the joint probability density function of the sampled data given the DoA's and viewed as a function of the desired variables which are the DoA's in this case. The operation principal of this method is to search for the directions that maximize the log of the likelihood function. The ML criterion signifies that plane waves from these directions are most likely to cause the given samples to occur. The MLM gives a superior performance compared to other methods, especially, at low SNR, number of samples is small or the sources are correlated, therefore, it is of practical interest [5].

The problem of maximizing the log-likelihood function is of a non-linear nature. To solve such a problem, iterative schemes should be utilized. Many schemes are available in the literature. One of them is the gradient decent algorithm using the estimated gradient of the function at each iteration. Another scheme is the Newton-

Raphson method. Other schemes such as the alternating projection (AP) method and the expectation maximization algorithm have been proposed for solving this problem. For the case of a single source, which is the case in this thesis, the estimates obtained by MLM are asymptotically unbiased. This means that the expected values of the estimates are equal to their true values. Hence, this method could be used as a standard to assess the performance of other DoA methods.

It has been shown that the MLM is a computationally extensive method; however, it is the optimum method in determining the DoA. It attains optimality as the number of elements in the array approaches infinity. Infinite number of elements in the array structure is not practical; therefore, the number of elements in the linear array is going to be limited to a maximum of 5 elements. Limiting the number of elements in the array structure leads to simpler and more efficient computations. The MLM would not be optimum anymore because the number of elements is not large enough to approach infinity. As far as this research is concerned, the signal processing side for determining the DoA is of less importance than the antenna design side. Another important point is that more optimum methods, such as MUSIC, for limited number of array elements are based on the Maximum Likelihood principle and, therefore, the MLM is going to be used and the principle is applicable to any other DoA estimation technique whether it is the optimum or not.

### ***3.1 Theoretical Background***

This section introduces the theory behind the MLM for DoA estimation. The mathematical derivation is for the general case in which more than one signal could be incident on the array structure at the same time.

The problem of finding the DoA using sensor arrays could be reduced to estimating the parameters in the following linear model:

$$y(t) = A(\theta)x(t) + e(t) \quad t = 1, 2, \dots, N. \quad (3.1a)$$

In (3.1a),  $y(t) \in C^{m \times 1}$  is the noisy data vector, where  $m$  is the number of array elements,  $x(t) \in C^{n \times 1}$  is the vector of signals amplitudes, where  $n$  is the number of signals,  $e(t) \in C^{m \times 1}$  is an additive noise, and the matrix  $A(\theta) \in C^{m \times n}$  has the following structure:

$$A(\theta) = [a(\omega_1) \dots a(\omega_n)] \quad (3.1b)$$

where  $\{\omega_i\}$  are real parameters,  $a(\omega_i) \in C^{m \times 1}$  is a so called transfer vector between the  $i^{\text{th}}$  signal and  $y(t)$ , and  $\theta = [\omega_1 \dots \omega_n]^T$ .

Some assumptions are made before further proceeding in the analysis of the model in (3.1):

- 1- The number of signals  $n$  incident on the array is known.
- 2- Once an estimate of  $\theta$  is available, the estimation of the signal amplitudes  $x(t)$  reduces to a simple mean square fit and they are considered as deterministic variables. The main objective is to determine  $\theta$ .
- 3-  $m > n$ , and the vectors  $a(\omega)$  corresponding to  $(n+1)$  different values of  $\omega$  are linearly independent.
- 4-  $Ee(t) = 0$ ,  $Ee(t)e^*(t) = \sigma I$  and  $Ee(t)e^T(t) = 0$ .
- 5-  $Ee(t)e^*(s) = Ee(t)e^T(s) = 0$  for  $t \neq s$  and  $e(t)$  is Gaussian distributed.



The log-likelihood function of the observations  $\{y(t)\}_{t=1}^N$  is given by:

$$L(y(1), \dots, y(N)) = \frac{1}{(2\pi)^{mN} (\sigma/2)^{mN}} \exp \left\{ -\frac{1}{\sigma} \sum_{t=1}^N [y(t) - Ax(t)]^* \cdot [y(t) - Ax(t)] \right\} \quad (3.2a)$$

$$L = \text{const} - mN \ln \sigma - \frac{1}{\sigma} \sum_{t=1}^N [y(t) - Ax(t)]^* \cdot [y(t) - Ax(t)] \quad (3.2b)$$

This function can be concentrated with respect to  $\sigma$ , and  $\{x(t)\}$ . Some straight forward calculations show that the ML estimators of these parameters are given by:

$$\hat{x}(t) = [\hat{A}^* \hat{A}]^{-1} [\hat{A}^* y(t)] \quad t = 1, \dots, N \quad (3.3)$$

$$\begin{aligned} \hat{\sigma} &= \frac{1}{mN} \sum_{t=1}^N [y(t) - \hat{A}\hat{x}(t)]^* [y(t) - \hat{A}\hat{x}(t)] \\ &= \frac{1}{m} \text{tr} [I - \hat{A}(\hat{A}^* \hat{A})^{-1} \hat{A}^*] \hat{R} \end{aligned} \quad (3.4)$$

where  $\hat{A}$  denotes the ML estimate of  $A$  (i.e.,  $\hat{A} = A(\hat{\theta})$ ), where  $\hat{\theta}$  is the ML estimate of  $\theta$ . Inserting (3.3) and (3.4) (with  $\hat{A}$ , which is not yet determined, replaced by  $A$ ) into (3.2b), we obtain the concentrated likelihood function:

$$const - mN \ln F(\theta)$$

where

$$F(\theta) = tr[I - A(A^* A)^{-1} A^*] \hat{R} \quad (3.5)$$

Therefore, the ML estimate of  $\theta$  is given by the minimizer of  $F(\theta)$  [1], [2].

Due to the assumptions made in this thesis, which are mentioned in chapter 6, the ML algorithm was further simplified and its computational complexity was reduced considerably. The ML algorithm was reduced to a one-to-one mapping problem between the DoA and the current samples taken from the array elements.

To describe the principal of operation of this method in a simple manner, one should look at it as follows:

- 1- Define a range of angles from which the incident signal is expected to arrive with a given resolution.
- 2- Create a look up table that includes sampled data from signals incident from the above specified range taken from the array elements.
- 3- Create an incident signal from an arbitrary angle but from within the defined range.
- 4- Add uncorrelated complex additive white Gaussian noise samples to the incident signal samples.
- 5- Correlate the data sampled from the incident signal with the data saved previously in the look up table and find the maximum correlation value and its corresponding DoA.

The linear array elements are viewed as sensors which sample the incident signal at various locations. Each sample consists of amplitude and phase. In order to have a better performance, more samples should be taken and; therefore, the number of elements in the array should be increased. And this is how the MLM attains optimality.

So far, the issue of mutual coupling hasn't been introduced yet. This chapter is concerned with the ideal case, in which mutual coupling doesn't exist between the elements of the array in order to see the abilities of the MLM in determining the DoA and the effect of changing certain parameters, such as the number of elements, elements pattern and spacing between the elements, on the performance of the estimator.

The next step would be to implement the MLM and compare the performance of different array structures.

First, the algorithm is going to be implemented for a 3-element linear array and a 5-element linear array in which the array elements are isotropic elements placed along the x-axis.

Second, the algorithm is going to be implemented for a 3-element linear array and a 5-element linear array in which the array elements are  $\lambda/2$  dipole antennas placed along the x-axis as shown in figure 3.1.

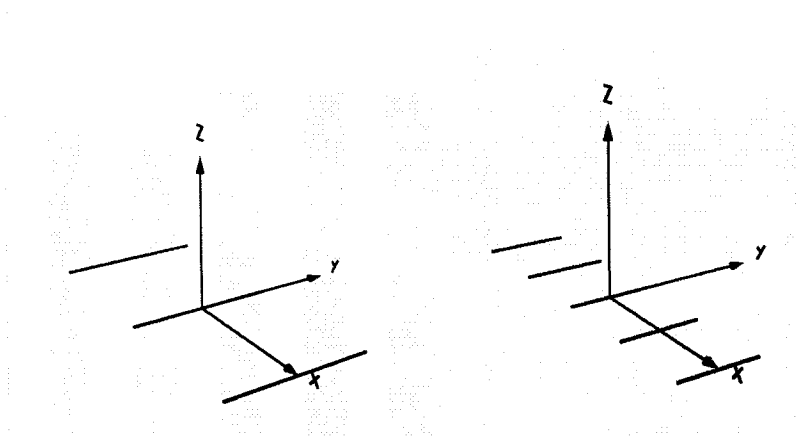


**Figure 3.1:** 3-element and 5-element  $\lambda/2$  dipole linear arrays geometry

Figure 3.1 shows the geometry of the array antennas used in the simulations to investigate the performance of the MLM as the number of elements change, the spacing between the elements change, or the elements pattern change.

The following assumptions hold throughout this section unless mentioned otherwise:

- 1- There is one incident signal at a time, no multiple signals considered.
- 2- The incident signal is at  $\theta = 30^\circ$  measured from the z-axis.
- 3- The look up table is defined from  $10^\circ$  to  $70^\circ$  with a step of  $0.5^\circ$ .
- 4- The incident signal is a function of  $\theta$  only, whereas  $\phi$  is held constant at  $0^\circ$ .
- 5- The array elements are placed  $\lambda/2$  apart.

To assess the performance of the MLM, one needs to identify how accurate this method is in determining the DoA of the incident signal. One possible option would be to calculate the Mean Square Error (MSE) resulting from estimating the Direction of Arrival (DoA). To do that, the number of runs needed to estimate the MSE accurately should be calculated. The following subsection includes how the word accurately could be quantified statistically.

### 3.2 *Statistical Analysis for Determining MSE*

Determining the Mean Square Error as a measure of performance of the MLM requires the determination of the number of times the experiment of determining the DoA should be run in order to determine MSE accurately. In other words, we need to determine the number of experiments needed so that the MSE will fall in a given range or interval. This range or interval is referred to as a confidence interval. The derivation for how to estimate the number of experiments needed to obtain a confidence interval for the parameter to be estimated is rather simple and could be found in any basic statistical analysis book [27]. In simple words, the number of runs necessary to be  $x\%$  confident that the error in estimating MSE will be less than a specified amount  $e$ , is given by the following equation:

$$n = \left( \frac{(t_{\alpha/2} \times S)}{e} \right)^2 \quad (3.6)$$

$S$  is the standard deviation of the data and  $t$  is dependent on the  $x\%$  value. Since  $S$  is unknown, it was estimated experimentally. The experiment of estimating MSE was run 1000 times, at the lowest SNR—i.e. maximum error, to find one value of MSE and this process was repeated 1000 times at  $\text{DoA} = 30^\circ$  for the two cases.

The choice of  $e$  is left as a design parameter and it varies according to the application.  $e = 0.0001$  was chosen for this study and the lowest SNR is 0 dB. The next step is to evaluate  $n$  for a 3-element linear array and 5-element linear array. The following results show the number of runs needed to be 95% confident that the error,  $e$ , will not exceed 0.0001.

1- 3-element linear array

$$S = 0.0026$$

$$n = \left( \frac{(1.96 \times 0.0026)}{0.0001} \right)^2 = 2596.5$$

Hence, the number of runs needed is 2597 runs.

2- 5-element linear array

$$S = 0.0012$$

$$n = \left( \frac{(1.96 \times 0.0012)}{0.0001} \right)^2 = 553.19$$

Hence, the number of runs needed is 554 runs.

At this point, we know the number of runs needed to be 95% confident that the error will not exceed 0.0001. A three trial run for the 3-element linear array and the 5-element linear array was performed according to the above obtained results and the following was found:

- 3-element linear array, 2597 runs, 3 trials.

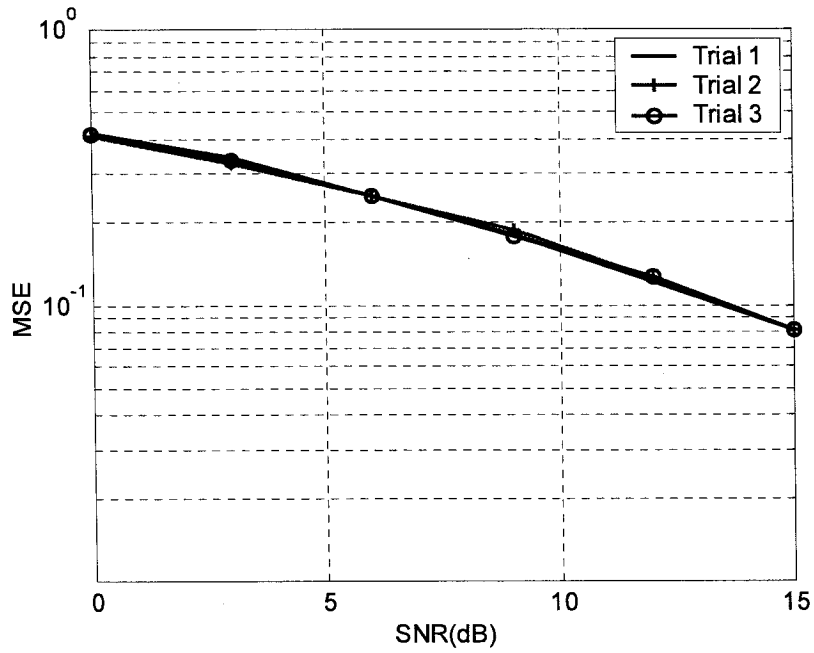


**Figure 3.2:** Three trial run for the 3-element linear array

It is clear, from figure 3.2, that the three trial run results obtained from running the algorithm for 2597 times produced almost identical results. The variation between the three MSE results is very small and would be less than 0.0001 in 95% of the cases.

- 5-element linear array, 554 runs, 3 trials.

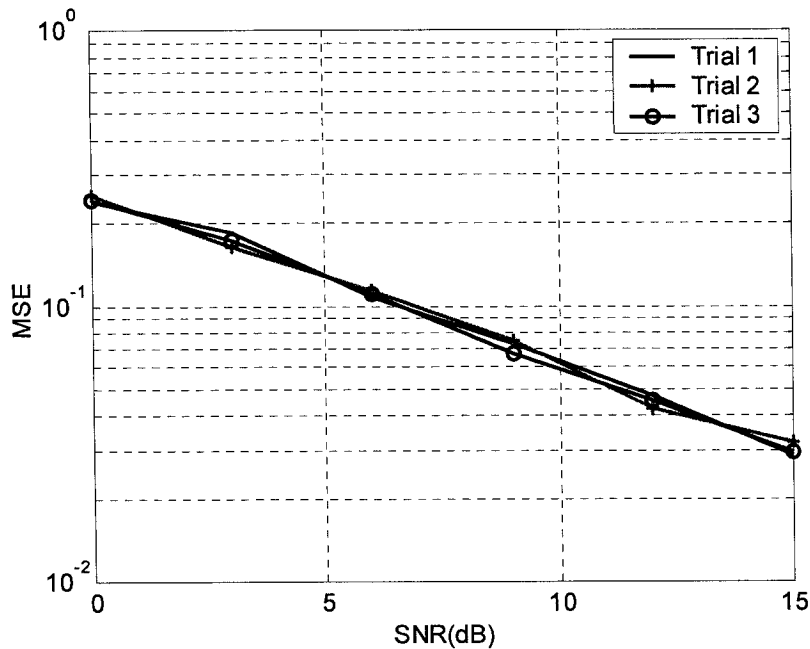


**Figure 3.3:** Three trial run for the 5-element linear array

Figure 3.3 is similar to figure 3.2. The three trial run results obtained from running the algorithm for 554 times produced almost identical results. The variation between the three MSE results is very small and would be less than 0.0001 in 95% of the cases.

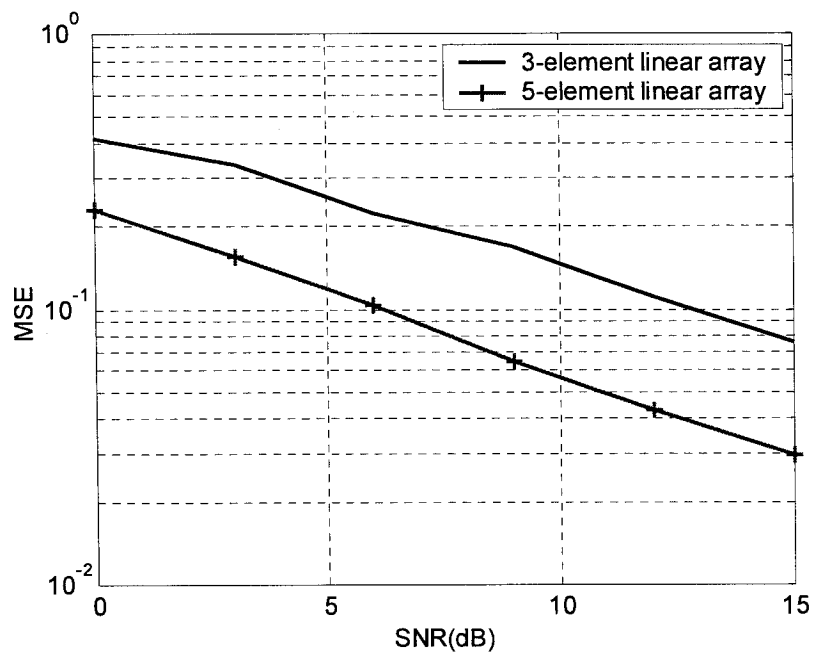
From the above results shown in figures 3.2 and 3.3, it can be concluded that if we run 100 trials of the 3-element and 5-element linear array estimation simulations, the error  $e$  will not exceed 0.0001 in 95 times and it will exceed 0.0001 in 5 times. It is impossible to predict the occurrence of 5 times ahead of time; otherwise it could have been avoided. The number of runs utilized to estimate the standard deviation of the data was sufficient to give a very accurate representation of the behavior of MSE. At each point of SNR, there could be constructed an interval—i.e. confidence interval,



in which the MSE will oscillate. The length of the interval is 0.0002. MSE with not overshoot this interval from either sides except in the 5% error case.

The complex additive white Gaussian noise samples of each experiment are uncorrelated—i.e. for the 3-element linear array, the MSE performance simulations are run 2597 times and uncorrelated complex additive white Gaussian noise is generated 2597 times.

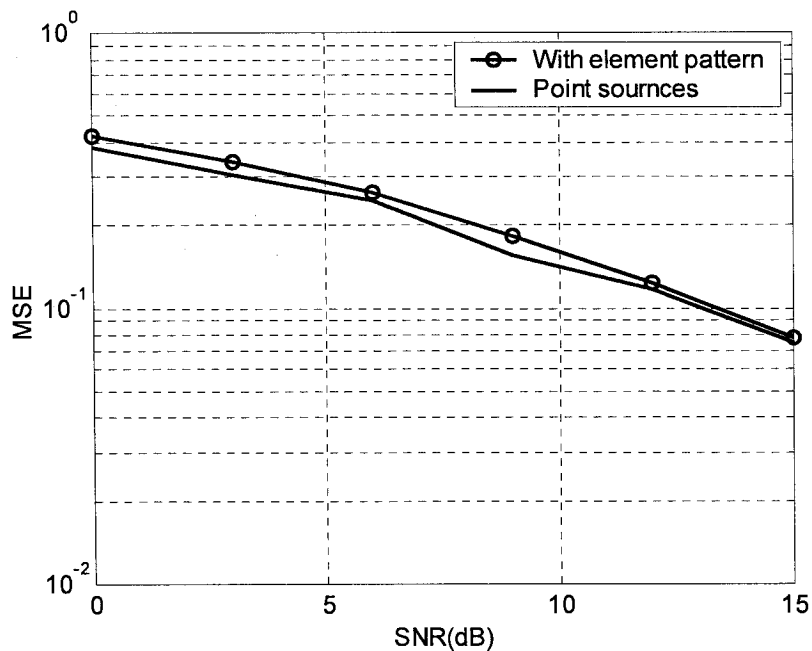
Having this done, the MLM can be implemented to estimate the DoA for the first case in which the array elements are point sources. This case represents the ideal case that DoA estimation techniques consider when their performance is studied. No mutual coupling between the elements is taken into consideration.



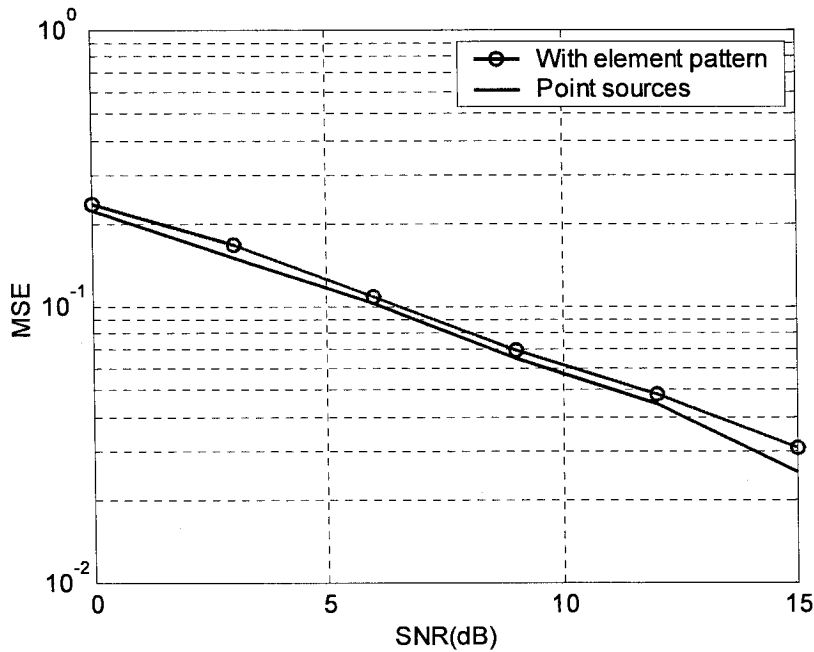
**Figure 3.4:** Comparison, in terms of MSE, between a 3-element linear array and a 5-element linear array

Figure 3.4 shows a comparison in performance of a 3-element linear array and a 5-element linear array. Increasing the number of elements resulted in more samples available for the MLM to estimate the DoA. It is clear that there is a gain of about 6 dB achieved when using a 5-element linear array instead of a 3-element linear array. Increasing the number of elements to more than 5-elements would further enhance the MSE performance as the MLM approaches optimality. The number of elements that could be used in the structure of the array antenna depends on the application, financial budget, and space available.

The next step would be to determine the MSE performance of the MLM when the elements used are half wave-length dipole antennas. No mutual coupling is considered.



**Figure 3.5:** Comparison, in terms of MSE, between a 3-element linear array with and without element pattern (dipole) included



**Figure 3.6:** Comparison, in terms of MSE, between a 5-element linear array with and without element pattern (dipole) included

Figures 3.5 and 3.6 show how the performance would change when more practical elements, such as dipole antennas, are used instead of the point sources. The performance is degraded with almost less than 1 dB in both cases. From a performance point of view, such degradation is negligible. This behavior could be explained by looking at the two linear arrays geometry shown in figure 3.1. The incident signal is arriving from  $\phi = 0^\circ$  and  $\theta = 30^\circ$  which means that, both, the isotropic element and the dipole antenna would have their maximum of the radiation pattern in the direction of the incident signal. In fact, as long as  $\phi = 0^\circ$ , both elements would perform similarly. If  $\phi$  is changed to  $90^\circ$  for instance, the performance of the linear array with dipole antennas as the array elements would be degraded considerably because part of the incident signal would arrive at the null of

the radiation pattern of each element. From this point, element pattern (dipole) is included in all the simulation results.

Another point of interest would be changing the spacing between the elements. As mentioned above in the assumptions, the spacing between the elements in the previous simulations was  $\lambda/2$ .

Since the incident signal is creating progressive phase between the array elements, and in order to avoid creating grating lobes when the spacing is changed, one must follow equation 3.7 to determine the maximum spacing  $d$  available for operation.

$$d \leq \frac{\lambda}{1 + |\cos \theta_0|} \quad (3.7)$$

Hence,  $d \leq (0.745) \lambda$ . One possible value to choose would be  $(0.6) \lambda$ .

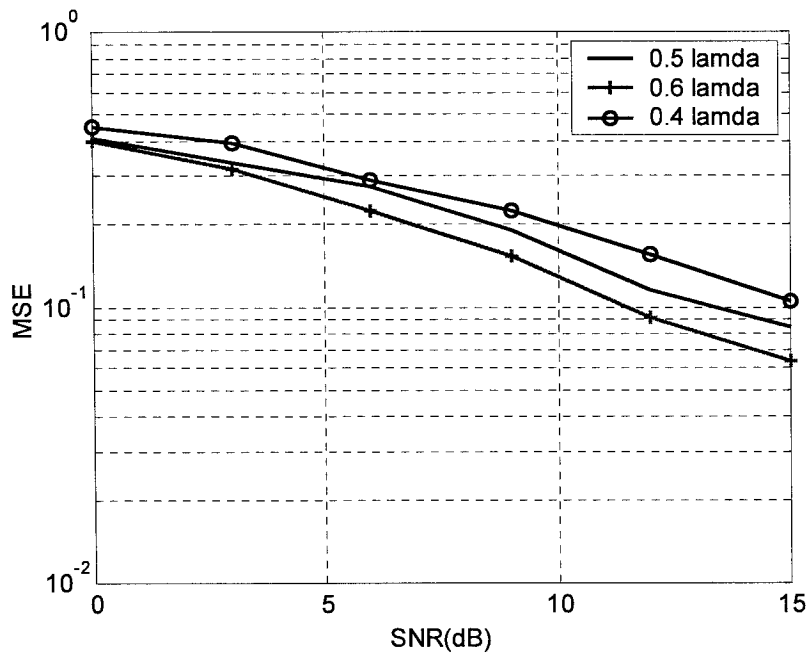


**Figure 3.7:** Changing the spacing between the elements for a 3-element linear array

Figure 3.7 shows that the performance is enhanced when the spacing between the array elements is increased. The amount of enhancement increases as SNR increases to reach almost 2.5 dB.

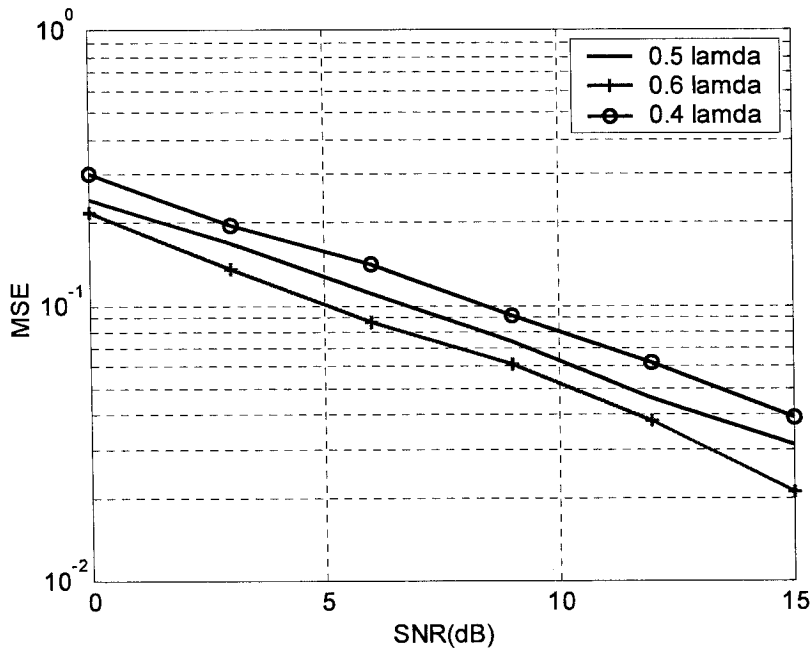


**Figure 3.8:** Changing the spacing between the elements for a 5-element linear array

Figure 3.8 also shows that the performance is enhanced when the spacing between the array elements is increased. There is a gain of about 2.5 dB achieved when using  $0.6 \lambda$  spacing between the elements.

These results show that the performance of the linear array in estimating the DoA is enhanced when the spacing between the elements is set to  $0.6 \lambda$ , and is degraded when the spacing is set to  $0.4 \lambda$ . The explanation for such behavior is that when the spacing between the elements is reduced, the phase difference between the signals picked—i.e. samples, at each element is reduced too, and with the addition of noise, it becomes harder for the estimator to differentiate between the phases and therefore estimate the DoA accurately. The same explanation applies when the

spacing between the elements is increased. The phase difference between the signals picked up—i.e. samples, at each element is increased and therefore, with the addition of noise, it is still easier to estimate the exact phase of the arriving signal and hence the DoA.

The Maximum Likelihood Method (MLM) showed great potential in determining the direction of arrival (DoA) of one incident signal on a linear array of 3 and 5 elements. As the number of elements was increased, more sample data was available to determine the DoA and; therefore, the performance was enhanced or in other words, the MLM started to approach optimality. For the above particular case, the performance with point sources or dipole antennas was similar, however, as soon as  $\phi$  changes; this performance would change depending in the choice of  $\phi$ . Increasing the spacing  $d$  between the elements resulted in a better performance since the phase of the sampled data has been further separated and hence, the dynamic range for the phase variation was increased.

## Chapter 4

### NEC2, Method of Moments, and Mutual Coupling

Numerical Electromagnetic Code NEC2 is a widely used software in antenna modeling and analysis of EM problems. It has been developed at the Lawrence Livermore Laboratory, Livermore, California, under the sponsorship of the Naval Ocean Systems Center and the Air Force Weapons Laboratory [28].

The principal of this code is to find a numerical solution of integral equations for the induced currents. These currents could be the result of an incident plane wave of a linear or elliptical polarization, or a voltage source connected to a wire. This code is capable of analyzing the electromagnetic response for an arbitrary structure consisting of wires and surfaces in free space or over a ground plane. The electromagnetic response includes current and charge density, near electric or magnetic fields, and radiated fields. The integral equation used is for smooth surfaces with one specialized to wires. That provides accurate and convenient modeling for a wide range of structures [28]. In the modeled structure, one can include non-radiating networks and transmission lines to connect different parts of the structure, perfect or imperfect conductors, and lumped-element loading. In addition to that, the structure may include perfect or imperfect ground plane.

The integral equations NEC2 uses are electric-field integral equation (EFIE) and magnetic-field integral equation (MFIE). The EFIE is used for thin-wire structures of very small volume. It can also be used to model surfaces in which there

is a thin structure and there is a little separation between the back and front surfaces. When the EFIE is used to model surfaces, these surfaces are represented by a wire grid. The MFIE is used for structures with relatively large volume especially those with smooth surfaces. In cases where structures contain wires and surfaces, both EFIE and MFIE are used together to determine the electromagnetic response. The full derivation of the EFIE and the MFIE and how they are used in NEC2 could be found in [28].

#### ***4.1 Method of Moments***

As mentioned previously, NEC2 is based on finding a numerical solution of integral equations for the induced currents on a structure. The Method of Moments (MoM) is used to find this numerical solution. The main concern of this thesis is directed towards wire antennas, to be more precise,  $\lambda/2$  dipole antennas. Therefore, the solution for the integral equation is going to be focused on the special case of finite diameter wires [25]. This subsection gives an overview on the integral equations and their MoM solution.



### 4.1.1 Pocklington's Integral Equation

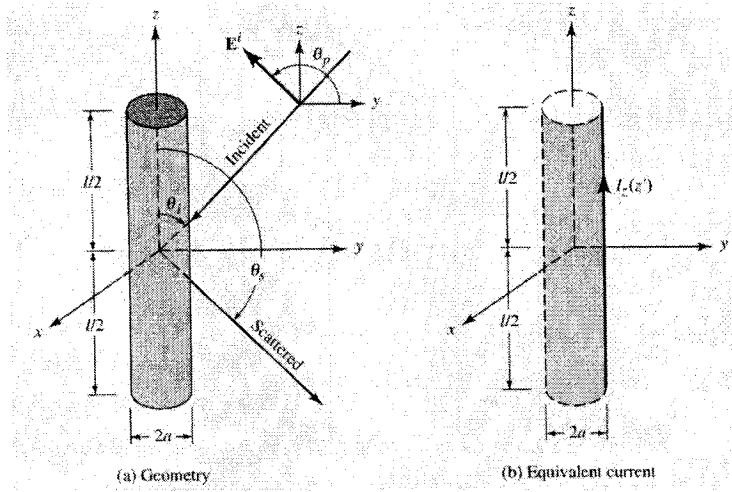


**Figure 4.1:** Uniform plane wave obliquely incident on conducting wire [25]

The *Pocklington's integral equation* for a dipole antenna shown in figure 4.1 is given by equation (4.1):

$$\int_{-l/2}^{+l/2} I_z(z') \left[ \left( \frac{\partial^2}{\partial z^2} + k^2 \right) G(z, z') \right] dz' = -j\omega\epsilon E_z^i(\rho = a) \quad (4.1)$$

where  $G(z, z') = \frac{1}{2\pi} \int_0^{2\pi} \frac{e^{-jkR}}{4\pi R} d\phi'$ ,  $k$  is the wave number,  $a$  is the radius of the wire

antenna, and  $R$  is the distance from the wire segment under consideration to the observation point.

When the incident field on the surface of the wire is known, equation (4.1) can be used to determine the equivalent filamentary line-source current of the wire and; hence, the current density on the wire.

If the wire is assumed to be very thin –i.e.  $a \ll \lambda$ , then the equation describing  $G(z, z')$  reduces to:

$$G(z, z') = G(R) = \frac{e^{-jkR}}{4\pi R} \quad (4.2)$$

Hence, equation (4.1) can be expressed as:

$$\int_{-l/2}^{+l/2} I_z(z') \frac{e^{-jkR}}{4\pi R^5} \left[ (1 + jkR)(2R^2 - 3a^2) + (kaR)^2 \right] dz' = -j\omega\epsilon E_z^i(\rho = a) \quad (4.3)$$

For observation along the center of the wire ( $\rho = 0$ ):

$$R = \sqrt{a^2 + (z - z')^2} \quad (4.4)$$

$I_z(z')$  in equations (4.1) and (4.3), represents the equivalent filamentary line-source current mentioned above. This current is located on the surface of the wire as shown in figure 4.1(b). It is obtained by knowing the incident electric field on the surface of the wire [25].

#### 4.1.2 Hallen's Integral Equation

In the dipole antenna shown in figure (4.1), lets assume that ( $l \gg a$ ) which implies that the length of the cylinder is much larger than its radius keeping in mind that ( $a \ll \lambda$ ) so that the effects of the end faces of the cylinder can be neglected.

Therefore, the boundary conditions for a wire with infinite conductivity are those of vanishing total tangential  $\mathbf{E}$  fields on the surface of the cylinder and vanishing current at the ends of the cylinder [ $I_z(z' = \pm l/2) = 0$ ] [25].

*Hallen's integral equation* is given by:

$$\int_{-l/2}^{+l/2} I_z(z') \frac{e^{-jkR}}{4\pi R} dz' = -j \sqrt{\frac{\epsilon}{\mu}} [B_1 \cos(kz) + C_1 \sin(k|z|)] \quad (4.5)$$

where  $a \ll \lambda$  here  $C_1$  and  $B_1$  are constants determined from applying a voltage source at the input terminals of the wire and applying the boundary condition that requires the current to vanish at the end points of the wire respectively.

#### 4.1.3 Method of Moments Solution

Equations (4.1), (4.3), and (4.5) are of the form:

$$\mathbf{F}(\mathbf{g}) = \mathbf{h} \quad (4.6)$$

where  $\mathbf{F}$  is a known linear operator,  $\mathbf{h}$  is a known excitation function, and  $\mathbf{g}$  is the response function. For (4.1),  $\mathbf{F}$  is an integrodifferential operator while for (4.3) and (4.5) it is an integral operator. The objective is to determine  $\mathbf{g}$  once  $\mathbf{F}$  and  $\mathbf{h}$  are specified.

The moment method technique represents the unknown response function  $\mathbf{g}$  as a linear combination expansion of  $N$  terms as:

$$g(z') = \sum_{n=1}^N a_n g_n(z') \quad (4.7)$$

$g_n(z')$  is a known function referred to as a basis or expansion function and the  $a_n$ 's are unknown constants.

Substituting (4.7) into (4.6), and based on the linearity of the  $F$  operator, (4.6)

becomes:

$$\sum_{n=1}^N a_n F(g_n) = h \quad (4.8)$$

The expression in (4.8) consists of  $N$  unknowns ( $a_n, n = 1, 2, 3, \dots, N$ ). In order to find these unknowns, it is necessary to have  $N$  linearly independent equations. The way to do this is by applying the boundary conditions at  $N$  different points. This process is called point-matching or collocation [25].

After performing the point-matching, equation (4.8) becomes:

$$\sum_{n=1}^N I_n F(g_n) = h_m, \quad m = 1, 2, \dots, N \quad (4.9)$$

And in matrix form, equation (4.9) becomes:

$$[Z_{mn}][I_n] = [V_m] \quad (4.10)$$

Where

$$Z_{mn} = F(g_n) \quad (4.10.a)$$

$$I_n = a_n \quad (4.10.b)$$

$$V_m = h_m \quad (4.10.c)$$

Solving for the unknown coefficients,  $a_n$  or  $I_n$  becomes straight forward as follows:

$$[I_n] = [Z_{mn}]^{-1} [V_m] \quad (4.11)$$

This was a brief discussion about the history of NEC2, as well as the theory behind its operation. The full mathematical derivation of the *Pocklington's* and the *Hallen's integral equations* and the Method of Moments solution could be found in many text books and in the literature [25], [29]-[32].

## ***4.2 Method of Moments and Wire Array Antennas***

The major advantage that the Method of Moments provides when analyzing or designing wire array antennas over other classical methods is that it completely takes the effect of mutual coupling between the array elements into consideration. It also provides other important advantages such as, there is no need for any unrealistic assumptions for the current distributions on the array elements, and it gives the flexibility of exciting or loading the array elements at any point along their lengths [33].

### 4.3 *Wire Modeling Using NEC2*

The basic principal for wire modeling in NEC2 is straight segments division of the wire. When a wire is divided into a number of segments, each of these segments should be given the coordinates of its two end points and a specific radius. If the segment length is defined as  $\Delta$ , then a very important factor in the modeling would be the segment length relative to the wave length  $\lambda$ . Generally speaking,  $\Delta$  should be less than  $(0.1) \lambda$  at the operating frequency. Longer segments may be acceptable on long wires with no sudden changes while shorter segments,  $0.05 \lambda$  or less, may be needed in modeling critical regions of an antenna in case of curved wires. The size of the segments determines the resolution in solving for the current on the model since the current is computed at the center of each segment. Extremely short segments, less than about  $10^{-3} \lambda$ , should also be avoided since the similarity of the constant and cosine components of the current expansion leads to numerical inaccuracy. The wire radius,  $a$ , relative to  $\lambda$  is limited by the approximations used in the kernel of the electric field integral equation. Two approximation options are available in NEC2, the thin-wire kernel and the extended thin-wire kernel. In the thin-wire kernel, the current on the surface of a segment is reduced to a filament of current on the segment axis. In the extended thin-wire kernel, a current uniformly distributed around the segment surface is assumed. The field of the current is approximated by the first two terms in a series expansion of the exact field in powers of  $a^2$ . The first term in the series, which is independent of  $a$ , is identical to the thin-wire kernel while the second term extends the accuracy for larger values of  $a$ . Higher order approximation are not used because they would require excessive computation time. In either of these approximations, only currents in the axial direction on a segment are considered, and variations of the current around the

wire circumference are not allowed. The acceptability of these approximations depends on both the value of  $(a/\lambda)$  and the tendency of the excitation to produce circumferential current or current variation. Unless  $(2\pi a/\lambda)$  is much less than 1. The accuracy of the numerical solution for the dominant axial current is also dependent on  $\Delta/a$ . Small values of  $\Delta/a$  may result in extraneous oscillations in the computed current near free wire ends, voltage sources, or lumped loads. Use of the extended thin-wire kernel will extend the limit on  $\Delta/a$  to smaller values than are allowed with the normal thin-wire kernel. Studies of the computed field on a segment due to its own current have shown that with the thin-wire kernel,  $\Delta/a$  must be greater than about 8 for errors of less than 1%. With the extended thin-wire kernel,  $\Delta/a$  may be as small as 2 for the same accuracy. When the extended thin-wire kernel option is selected, it is used at free wire ends and between parallel, connected segments. However, the normal thin-wire kernel is always used at bends in wires. Hence, segments with small  $\Delta/a$  should be avoided at bends. Use of a small  $\Delta/a$  at a bend, which results in the center of one segment falling within the radius of the other segment, generally leads to severe error [24].

#### ***4.4 Mutual Coupling***

In this thesis, array elements behavior is going to be studied when plane waves are incident from different angles measured from the broad side and; therefore, mutual coupling will have a significant effect on the linear array performance. The issue of mutual coupling between array elements and the effect of changing the incident signal direction on it has been discussed in many papers before and its theory is well established in many books [25], [34], and [35].

In order to describe mutual coupling in simple words, it can be thought of as two antennas placed close to each other. Both can be receiving or transmitting simultaneously, or one is receiving and the other is transmitting. In such a situation, some of the energy that is directed to one of the antennas will end up on the other antenna. There are many factors that control this transfer of energy but the most important ones are:

- The spacing between the elements.
- The radiation pattern of each element.
- The relative orientation of each element with respect to the other elements.

One possible way to explain how the energy transfer could occur is by realizing that the radiation pattern of each antenna is not perfect—i.e. not exactly as designed theoretically. In the case where we have two transmitting antennas, some of the transmitted energy from one of the antennas will be received by the other one, and then re-scattered. This will affect the overall radiation pattern if we look at the two antennas at the same time as an array. The process of energy transfer and re-scattering is known as “Mutual Coupling”. In most applications, phased arrays are used because of their scanning abilities. The mutual coupling issue rises when the main lobe of the array is not at a fixed angle and it moves within a certain range. As described earlier, the change in the direction of the main lobe will change the number of array elements subject to the radiated energy and, therefore, will change the mutual coupling between the array elements. Mutual coupling can take place in the transmitting mode as well as the receiving mode of the array. Consequently, a quantitative estimation of the mutual coupling between the array elements as a function of the scanning angle is of great demand since it affects many parameters such as the radiation pattern of the array, the gain as well as the input impedance of the array.



### A. Transmit Mode

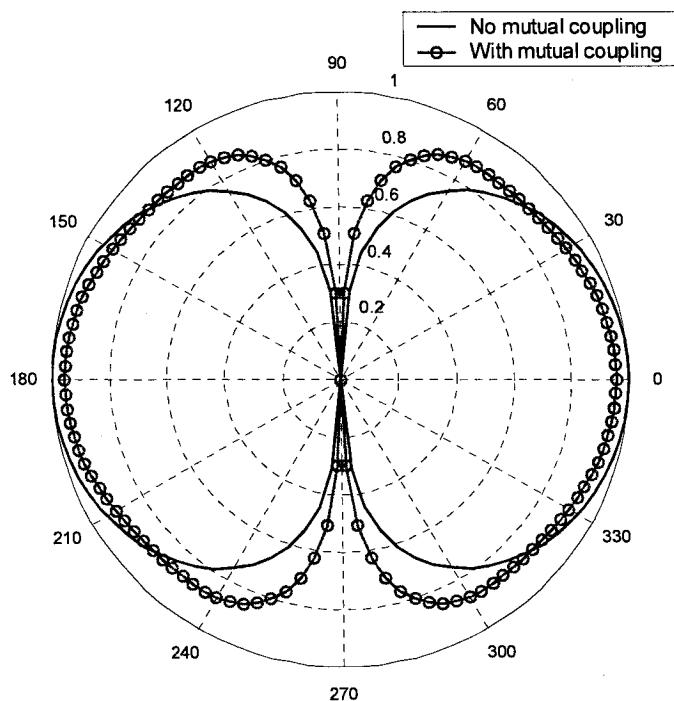


**Figure 4.2:** Illustration of the effect of mutual coupling

Figure 4.2, shows the radiation pattern of a  $\lambda/2$  dipole antenna placed along the y-axis at  $x = 0$  and it represents two cases. The first case is a  $\lambda/2$  dipole antenna in free space and it is represented by the solid line, we can see the conventional  $\lambda/2$  dipole antenna radiation pattern. The second case consists of three  $\lambda/2$  dipole antennas placed  $\lambda/2$  apart and oriented as a linear array in the xy plane. Only the center antenna is excited, and the other two antennas are not connected to a source. The radiation pattern is shown by the circle marked line. It can be noticed that, although only the center element is excited, the passive elements have contributed to the total radiation pattern because some of the energy transmitted from the center element was received

by the other two elements and then re-scattered. This illustrates the energy transfer principal mentioned earlier.

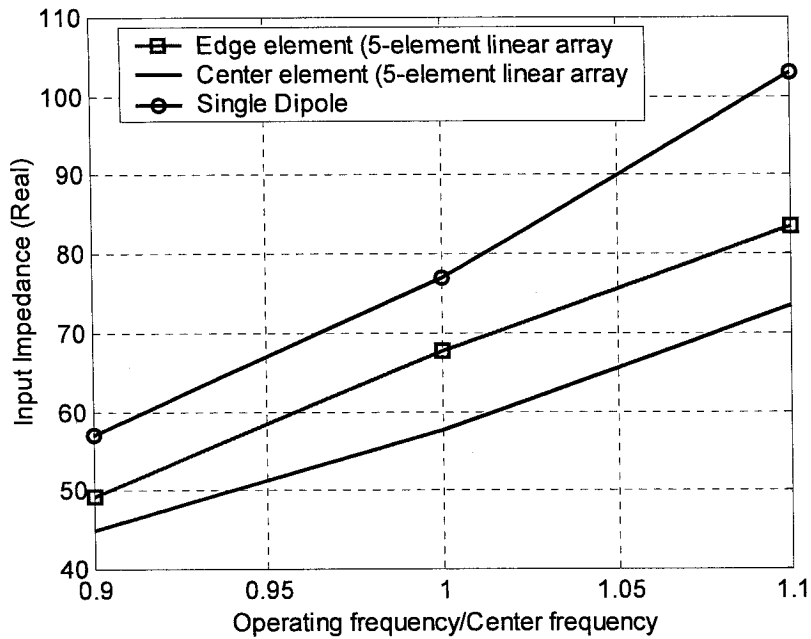
### *B. Receive Mode*

To look at the effect of mutual coupling in the receive mode, the following experiment was conducted and it consists of two parts:

The first part is a  $\lambda/2$  dipole antenna placed along the y-axis in the xy plane at  $x = 0$ , and the excitation was chosen to be a plane wave incident on this dipole from  $\theta = 10^\circ$  and  $\phi = 0^\circ$ . The current was sampled from the center segment of the antenna and it was  $3.7978 \times 10^{-3} \angle -28.306^\circ$ . The second part is three  $\lambda/2$  dipole antennas placed  $\lambda/2$  apart and oriented as a linear array in the xy plane, the center element is placed at  $x = 0$ . The array was excited by the same plane wave used in part one and the current of the center element was sampled at the center segment and it was  $6.1498 \times 10^{-3} \angle -1.885^\circ$ . In both cases, the current was sampled at the exact same location and from the exact same segment. The difference in the two readings is due to the effect of the other elements, in the second case, on the center element. This simple approach showed how mutual coupling affects the measurements taken and it illustrated that, in a practical system, mutual coupling exists and it should be accounted for in the design stage.

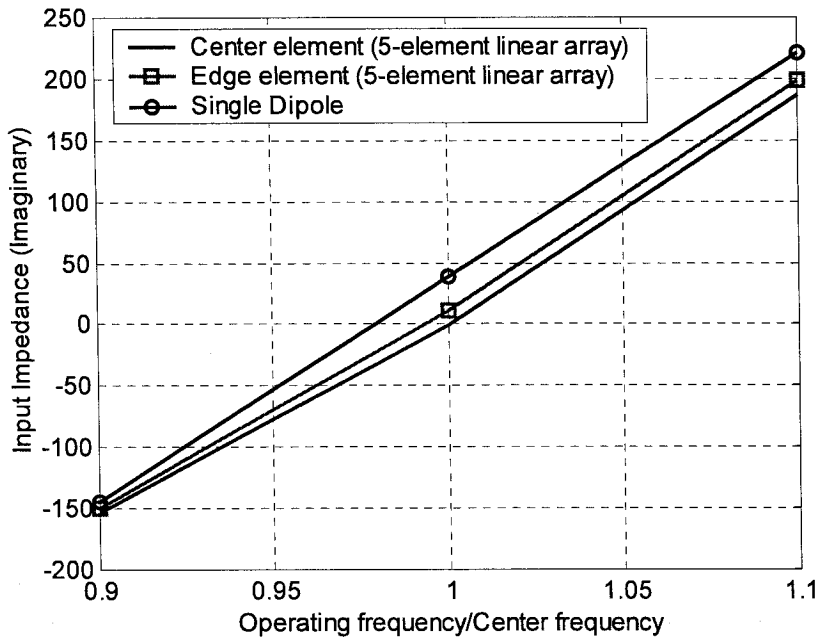
The input impedance of the array elements changes as a function of the operating frequency. In real life applications, the operating frequency is slightly different from the original design operating frequency  $f_o$  due to the frequency drift that occurs in the equipment. To see the effect of that drift on the input impedance of

the array elements, the input impedance performance is studied for operating frequencies of  $f_o$ ,  $0.9 f_o$  and  $1.1 f_o$ .



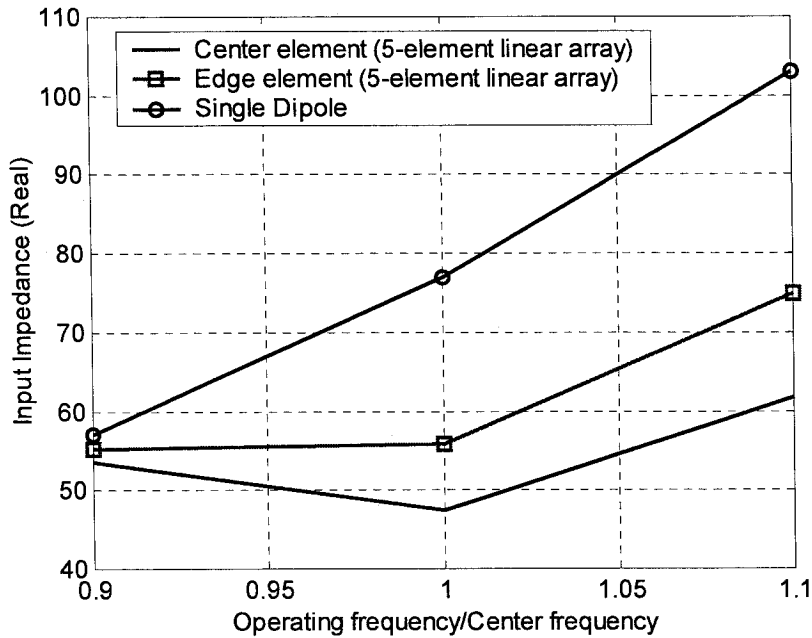
**Figure 4.3:** Real part of input impedance as a function of the operating frequency for a single dipole, center element and edge element of a 5-element linear array

Figure 4.3 shows the behavior of the real part of the input impedance of three cases. The first case is a simple  $\lambda/2$  dipole antenna, the second case is the center element of a 5-element linear  $\lambda/2$  dipole array antenna, and the third case is the edge element of a 5-element linear  $\lambda/2$  dipole array antenna. It can be noticed that the three lines in figure 4.3 are almost parallel and, for this specific range of frequency, the change in the input impedance could be described as a linear change.



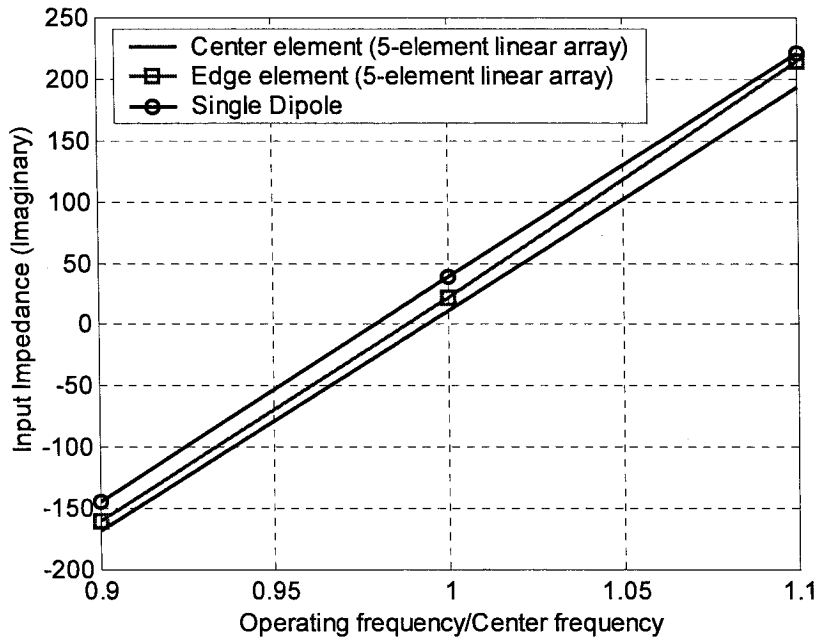
**Figure 4.4:** Imaginary part of input impedance as a function of the operating frequency for a single dipole, center element and edge element of a 5-element linear array

Figure 4.4 shows the behavior of the imaginary part of the input impedance of the three cases described above in figure 4.3. The three lines are almost parallel to which indicates that the change is almost linear in the input impedance as a function of the operating frequency.



**Figure 4.5:** Real part of input impedance as a function of the operating frequency for a single dipole, center element and edge element of a 5-element linear array with 0.6 lambda inter-element spacing

Figure 4.5 shows the behavior of the real part of the input impedance of the three cases described above except for one difference. The inter-element spacing in the 5-element linear  $\lambda/2$  dipole array antenna is  $0.6\lambda$  instead of  $0.5\lambda$ . The single dipole input impedance changes almost linearly whereas the input impedance of the center and the edge elements of the 5-element linear array tend to be close to each other at  $0.9f_o$  and then split further apart as the operating frequency is increased. It is going to be shown at a later stage of this thesis that changing the spacing between the array elements, subject to certain conditions, will enhance the MSE performance of the DoA estimation process.



**Figure 4.6:** Imaginary part of input impedance as a function of the operating frequency for a single dipole, center element and edge element of a 5-element linear array with 0.6 lambda inter-element spacing

Figure 4.6 shows the behavior of the imaginary part of the input impedance of the three cases described above in figure 4.5. The three lines are almost parallel too which indicates that the change is almost linear in the input impedance as a function of the operating frequency.

The effect of mutual coupling between the array elements on the performance of the array antenna extends to include the radiation pattern of the array antenna. This could be illustrated by plotting the radiation pattern of a 5-element linear  $\lambda/2$  dipole array antenna with and without taking mutual coupling into consideration. The elements are  $\lambda/2$  meters apart and the array is uniformly excited i.e.—uniform array. Uniform array means that the elements are identical, the excitation is of identical

magnitude, and the phase is progressive between the elements. In this case, the phase of the elements is chosen to be identical too in order to have the main lobe of the radiation pattern in the broadside direction of the array axis.

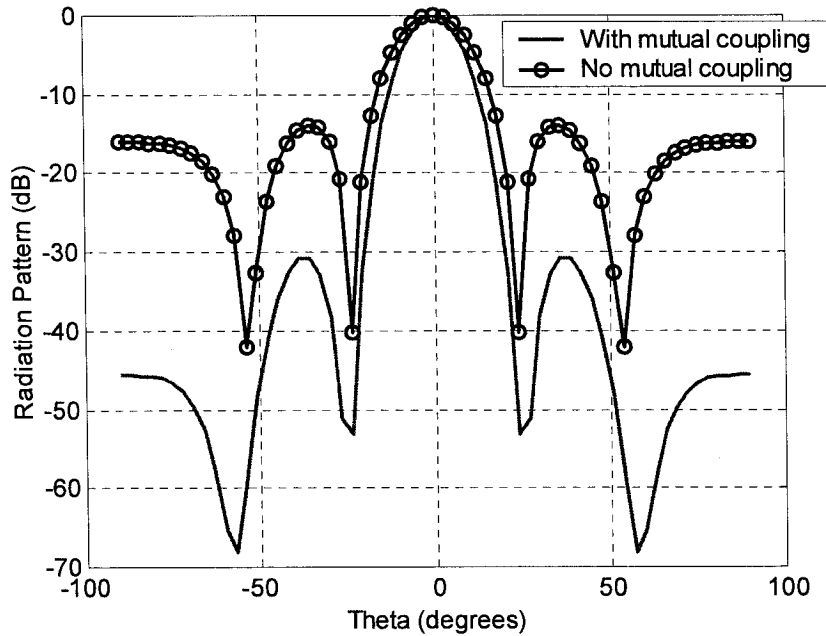


**Figure 4.7:** Radiation pattern of a 5-element linear  $\lambda/2$  dipole array antenna with and without mutual coupling

Figure 4.7 shows a comparison in the radiation pattern of a 5-element linear  $\lambda/2$  dipole array antenna with and without taking mutual coupling into consideration. There is a clear difference in the two radiation patterns due to the effect of mutual coupling between the array elements.

Theoretically speaking, the maximum of the first side lobe in a uniform array should be 13.46 dB below the maximum of the main lobe which is the case in the circle marked line. However; the solid line shows that the maximum of the first side lobe is more the 13.46 dB below the maximum of the main lobe. Therefore, the effect of mutual coupling between the array elements is an important factor that should be

taken into consideration when designing array antennas whether for DoA estimation purposes or not.

#### ***4.5 Summary and Illustrative Experiment***

Mutual coupling is becoming a very important aspect when we think about using array antennas, especially, scanning arrays. This importance is coming from the increasing demand on phased array antennas in many applications such as radar systems and MIMO communications systems. This section provided an over all idea on the definition of mutual coupling, how it occurs, and what makes it change.

In this thesis, we will be more concerned about the effect of mutual coupling between linear  $\lambda/2$  dipole array elements when the array is in the receiving mode. An experiment has been conducted to illustrate the effect of mutual coupling on DoA estimation process. First, the MLM was used to estimate the direction of arrival of a signal incident on a 5-element linear  $\lambda/2$  dipole array without taking mutual coupling into consideration. Second, the MLM was used to estimate the direction of arrival of a signal incident on a 5-element linear  $\lambda/2$  dipole array taking mutual coupling into consideration. The following assumptions are applied to the experiment:

- a) The incident wave is a function of theta only, whereas phi is held constant at  $0^\circ$ .
- b) The distance between each two elements is  $\lambda/2$  meters.
- c) The dipole antenna radius = 0.00001 meters.
- d) There is one incident signal at a time, no multiple signals considered.

The technique used to account for mutual coupling is based on integrating Matlab and NEC2 to form a DoA estimation system. Full details about the integration between the



two softwares are going to be provided in chapter 5. Figure 4.8 shows the ideal case in which no mutual coupling between the elements is taken into account.

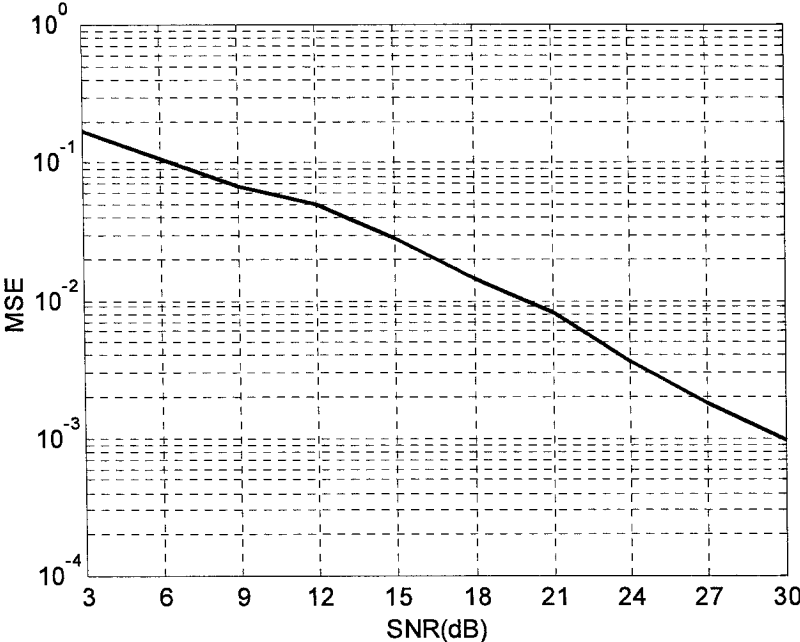


Figure 4.8: MSE for the MLM with no mutual coupling

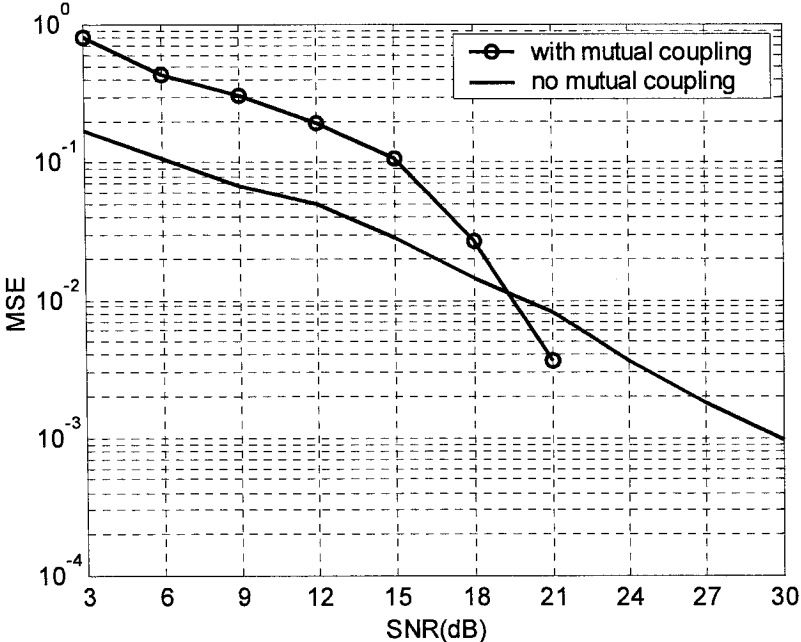


Figure 4.9: Comparison between the "without mutual coupling" case and the "with mutual coupling" case

Figure 4.9 shows the results for both cases. The MSE performance of the DoA estimation algorithm with no mutual coupling is better than the performance with mutual coupling until SNR reaches almost 19.5 dB. At higher SNR, the performance with mutual coupling becomes better and MSE reduces to zero at SNR higher than 21 dB. However, SNR as high as 21 dB, is not practical when wireless applications are considered. Therefore, SNR lower than 21 dB should be of more interest to us when we examine the performance. The performance was degraded of about 9 dB due to the effect of mutual coupling between the array elements. This experiment illustrates the severe effect of mutual coupling. Such an effect has been ignored in many DoA estimation research papers.

## Chapter 5

### Development of NEC2-Matlab Interface

#### 5.1 NEC2 Input/Output Files Format

As mentioned previously, in NEC2, the applied source can vary between a plane wave incident on the designed structure, or a delta-gap voltage source applied to a certain part of the structure. The advantage that this variation gives is the ability to study either the scattering or electromagnetic compatibility issues or the near field/far field radiation characteristics. Non-radiating structures can also be integrated with the antenna under investigation. Such structures include transmission lines, two-port networks, and lumped circuit networks. One major advantage that was of great significance in this thesis is the ability to introduce a ground plane in conjunction of the linear array antenna under investigation. This great significance is going to be obvious at a later stage of this report. In order to be able to integrate NEC2 and Matlab, one should be familiar with the input/output files format. The input to NEC2 is simply a text file that has a specific format. The name of the file could be of any choice –i.e. *filename.txt*. The output file is also a text file that could take any name specified by the user—e.g. *output.txt*. When NEC2 is run, the software asks the user to type a name for the input file which should be already created and saved in the same directory of NEC2. Then, NEC2 executes the input file and asks the user to enter a name for the output file which will be saved in NEC2 directory as well. The input and output files has certain format that should be followed in a very strict

manner. Detailed information about input files commands and column allocations as well as output file format could be found in [24].

## ***5.2 NEC2-Matlab Interface***

This section fully describes the purpose of integrating NEC2 and Matlab, and how these two softwares are integrated. NEC2 and Matlab are integrated in a way such that Matlab takes control of the DoA estimation process and produces Mean Square Error graphs for the DoA for different scenarios.

### ***5.2.1 NEC2-Matlab Interface Commands and Procedure***

Matlab gives great flexibility when dealing with input and output imported from and exported to other workspaces. When NEC2 is run in Windows environment, it utilizes a Command Prompt window to instruct the user to enter a name for the input and output files. Matlab can invoke an operating system command by using "!" followed by the NEC2 in this case to run it automatically from Matlab. However, since NEC2 requires the user to specify the names of the input and output files manually, it was impossible to do that using Matlab. Therefore, some changes to NEC2 source code were necessary in order to make it compatible with Matlab. These changes are the following:

1. The name of the input file is always fixed to nec.inp, this name doesn't change.
2. The output file is sub-divided into several files each represents one part of the original output file.
  - a. The full output file is named "nec.out".

- b. The radiation pattern data is named "nec.pat".
- c. The current at each segment on the wire structure is named "nec.cursor".

These file names are fixed and the need of manual user entry for these names is eliminated. At this point, when Matlab calls NEC2, NEC2 will automatically look for a file named "nec.inp" to take it as an input file. Consequently, it will produce three output files. All files are in the same directory of NEC2. Each time the input file is changed, it will over write the previous input file.

Matlab has the ability to write any specified data or text in a text file and save it under a name specified by the user. In this case, the name is going to be "nec.inp" for all input files. The commands that are used to perform this task in Matlab are "fopen" and "fprintf". The command "fopen" specifies the file name and the permission. The permission in this case would be to write in this file. "fprintf" has a format string that contains C language conversion specifications. Conversion specifications involve the character %, optional flags, optional width and precision fields, optional subtype specifier, and conversion characters d, i, o, u, x, X, f, e, E, g, G, c, and s. The special formats \n, \r, \t, \b, \f can be used to produce linefeed, carriage return, tab, backspace, and form feed characters respectively. For complete details, one should refer to a C language manual.

Similar to the writing function, the reading function is composed of two commands. The first command is "fopen" and the second one is "fscanf". The function of "fopen" is to open the text file (output file) so that Matlab can read it. "fscanf" has a format string that contains C language conversion specifications. Conversion specifications involve the character %, optional assignment-suppressing

asterisk and width field, and conversion characters are d, i, o, u, x, e, f, g, s, c, and [. . .] (scanset). For instance, using %c means that Matlab will read the space characters, and %s means that it will skip all white space. For a complete conversion character specification, one should refer to a C language manual.

When Matlab reads the data from the output file, it saves it in an array whose size could be very large depending on the type of results NEC2 had produced. Using the array index, the user can eliminate all the un-needed data and use the remaining for further processing. After modifying NEC2 to produce the output file as a set of three files, this eliminating process became easier since the needed information is included in the nec.cursor file. Therefore, we can ignore the rest of the data in the other files.

The operational procedure that connects Matlab to NEC2 is described in the following steps:

1. Matlab creates an input text file named "nec.inp" for NEC2 that creates a 5-element  $\lambda/2$  dipole linear array shown in figure 2.1, with the source being a plane wave incident from a set of different angles (theta) whereas phi is held constant at zero degrees.
2. Matlab calls NEC2 and the input file is executed to produce an output of three text files.
3. Matlab reads the needed information from the output file "nec.cursor" and saves it in what is defined at a look up table which provides currents sampled from the center segment of each dipole in the array for further

processing. Since the array consists of 5 elements, each incident plane wave will result in a set of five current samples saved in the look up table.

4. Matlab creates another input file for NEC2 that creates a plane wave incident on the same structure created in step one, and it samples the currents from the center segment of the dipole antennas in the array. The angle of the incident signal could be a predefined angle in the look up table or a new angle that the system has not been trained on previously but from within the range of angles used in step 1. For example, if the range in step 1 is chosen to be from  $-10^\circ$  to  $10^\circ$  with a step of  $5^\circ$ , then we will have a set of 5 incident plane waves (not simultaneous) from  $-10^\circ$ ,  $-5^\circ$ ,  $0^\circ$ ,  $5^\circ$ , and  $10^\circ$ . The plane wave created in step 4 could be incident from  $\theta = 5^\circ$  – i.e. a predefined angle, or  $7^\circ$  – i.e. a new angle that the system has not been trained on.
5. Matlab takes the sampled data from step 4 and adds Complex Additive White Gaussian Noise to it.
6. Finally, Matlab uses the MLM on the sampled currents from step 5 and the samples saved in the look up table from step 3 in order to determine the DoA of the signal created in step 4.

From the above steps, one can realize that it is a very tedious, and almost impossible, exercise to sample the currents from the center segment of each dipole, for each incident plane wave, then save it in a look up table, sample the currents from the center segment of each dipole for the new incident plane wave, and then use all this sampled data to determine the DoA of the new incident plane wave. Therefore, the integration between Matlab and NEC2 is of great importance since it automates

the complete process and the user would just need to specify very few parameters in this process. It also solved the problem of iterative procedure to obtain the MSE by running each experiment up to 554 runs. Matlab also provides a rather simple environment for mathematical data processing and graphical display.



## Chapter 6

# NEC2/MLM Simulation Results and Element Selection

In the previous chapters, a solid discussion about the MLM, NEC2 and Matlab has been founded. Also, a full explanation about the integration process and its advantages between NEC2 and Matlab has been provided. The next step to take would be to test the integrated NEC2-Matlab system for different scenarios of plane waves incident on the linear array structure and study the effect of element selection on the DoA estimation system.

Before proceeding any further, the following assumptions are worth mentioning:

1. The array under consideration is a 5-element linear array shown in figure 3.1.
2. The incident wave is a function of theta only, whereas phi is held constant at  $0^\circ$ .
3. The elements of the array are  $\lambda/2$  dipole antennas and the distance between each two elements is  $\lambda/2$  meters.
4. The  $\lambda/2$  dipole antenna radius = 0.00001 meters.
5. There is one incident signal at a time, no multiple signals considered.

### ***6.1 Input Impedance of a $\lambda/2$ Dipole Antenna***

The input impedance, in its general form, could be defined as the impedance presented by an antenna at its terminals or the ratio of the voltage to current at a pair

of terminals or the ratio of the appropriate components of the electric to magnetic fields at a point [25]. The impedance of an antenna at its input terminals is of interest in this thesis and, therefore, it is going to be further explored.

The input impedance consists of real and imaginary parts. A typical  $\lambda/2$  dipole antenna has a radiation resistance, real part,  $R_r = 73$  ohms which is very close to the 75-ohm characteristic impedance of some transmission lines. In the case of a  $\lambda/2$  dipole antenna, the radiation resistance is also the input resistance at the input terminals of the  $\lambda/2$  dipole antenna because the current is maximum at the input terminals. The imaginary part, reactance, is a function of the dipole length and for a  $\lambda/2$  dipole antenna it is equal to  $j42.5$ . In practice, the main target would be to reduce the imaginary part of the input impedance and make it as close as possible to zero. This is achieved by reducing the length of the  $\lambda/2$  dipole antenna until the reactance vanishes.

In this thesis, the typical  $\lambda/2$  dipole antenna input impedance is used in all the simulations performed by the NEC2-Matlab integrated system. The value of  $73 + j42.5$  is going to be attained as close as possible. Figure 6.1 and 6.2 show the input impedance as a function of the dipole length over  $\lambda$  obtained from NEC2.

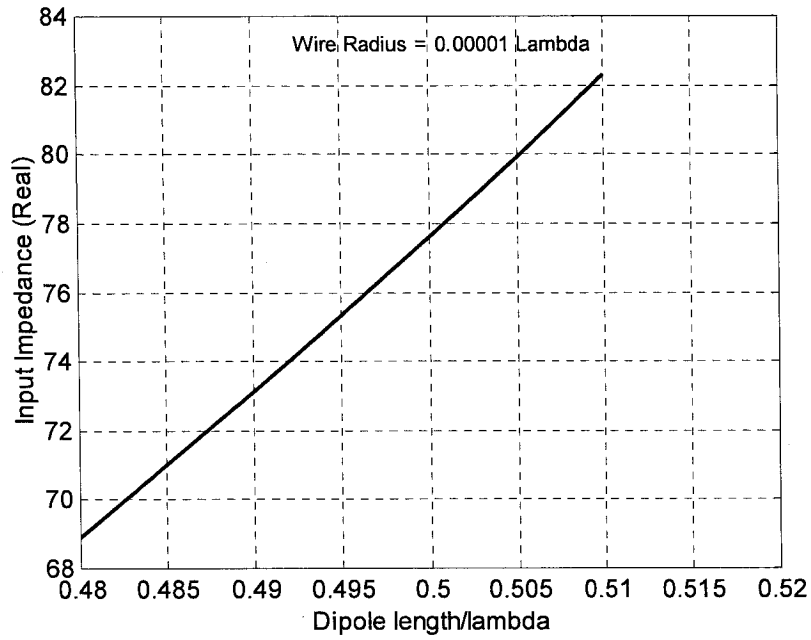


**Figure 6.1:** Input resistance of a center-fed  $\lambda/2$  dipole antenna as a function of its length

Figure 6.1 shows that the input resistance behaves almost linearly in the plotted region. The value of 73 is achieved at a length of  $0.49 \lambda$ . However, at  $0.49 \lambda$ , the input reactance shown in figure 6.2 is equal to 8 which is very far from 42.5.

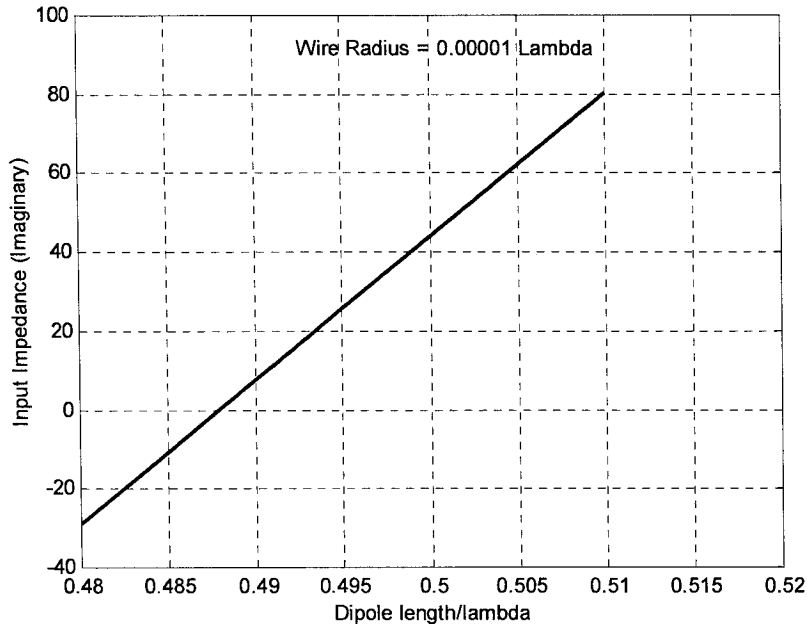


**Figure 6.2:** Input reactance of a center-fed  $\lambda/2$  dipole antenna as a function of its length

Figure 6.2 shows the input reactance of a center-fed  $\lambda/2$  dipole antenna as a function of its length. This figure in conjunction with figure 6.1 were used to determine the exact length of the  $\lambda/2$  dipole antenna in order to be as close as possible to  $73 + j42.5$ .

It was possible to reach a value of  $76.9 + j38.7$  by changing the length of the dipole antenna in order to get as close as possible to  $73 + j42.5$ . This input impedance was achieved at a length of  $0.4955 \lambda$ .

## ***6.2 $\lambda/2$ Dipoles and $\lambda/2$ Dipoles above Perfectly Conducting***

### ***Ground Plane***

As mentioned previously, most of the DoA estimation techniques available in the literature concentrate on the signal processing side and, somehow, pay less attention to the array antenna side. They assume either isotropic elements as the array elements or  $\lambda/2$  dipole antennas. This section suggests that the use of more directive elements in the array structure would enhance the performance of the MLM DoA estimation technique. The use of NEC2 as a major part of this thesis limits the choices of the elements that could replace the conventional  $\lambda/2$  dipole antennas. For example, micro-strip patches couldn't be modeled on NEC2 due to the lack of ability to introduce such new elements because there are no dielectric material definitions available. Therefore, a compromise between the conventional  $\lambda/2$  dipole antennas and the micro-strip patches was to use elements that NEC2 can construct and, at the same time, possess higher directivity than the conventional  $\lambda/2$  dipole antennas. The proposed new elements are  $\lambda/2$  dipole antennas above perfectly conducting ground plane. A  $\lambda/2$  dipole antenna above perfectly conducting ground plane has higher directivity than a  $\lambda/2$  dipole antenna in free space. Hence, an enhancement in the MSE performance is expected when such elements are deployed.

#### ***6.2.1 Approximation of a Micro-strip Patch***

A way to approximate a micro-strip patch is by using a horizontal dipole antenna above a perfectly conducting ground plane. However, the height at which the dipole is placed is not the same as the height of the dielectric material in the micro-strip patch because of the absence of the dielectric material and the presence of free

space instead. Although this is not an accurate representation of a micro-strip patch, it gives a rough estimate about the height at which the  $\lambda/2$  dipole antenna should be placed above the ground plane.

One of the commercial micro-strip substrate available has  $\epsilon_r = 2.5$  and  $h = 0.0016$  m. Let the distance between the dipole antenna and the ground plane be denoted by  $h'$ .

The effective dielectric constant of a micro-strip line is given by [36]:

$$\epsilon_e = \frac{\epsilon_r + 1}{2} + \frac{\epsilon_r - 1}{2} \frac{1}{\sqrt{1 + 12h/W}} \quad (6.1)$$

where,  $W$  is the width of the micro-strip line.

The term  $\frac{1}{\sqrt{1+12h/W}}$  becomes very small when applied to a dipole antenna since  $W$  is going to be very small. Therefore, we can ignore the whole term after the (+) sign.

$$\text{Hence, } \epsilon_e = \frac{2.5+1}{2} = 1.75.$$

$$\text{Since, } \lambda_e = \frac{\lambda_o}{\sqrt{\epsilon_e}} \quad (6.2)$$

$$\text{Then, } \lambda_e = 0.756\lambda_o$$

$$\text{If we assume that } \frac{h'}{\lambda_o} = \frac{h}{\lambda_e}, \text{ then } h' = 1.3229h$$

The new elements are going to be  $\lambda/2$  dipole antennas that are placed 0.00211 meters above the perfectly conducting ground plane.

### 6.2.2 *Maximum Directivity $D_o$*

Section 6.2.1 proposed the use of a dipole antenna above a perfectly conducting ground plane to approximate a micro-strip patch antenna as an alternative for more directive elements. To validate this approximation in terms of increased directivity, we would find the maximum directivity  $D_o$  for a  $\lambda/2$  dipole antenna in free space and for a  $\lambda/2$  dipole antenna above a perfectly conducting ground plane with  $h'$  specified above.

The maximum directivity for directional patterns [25] is expressed by:

$$D_o = \frac{4\pi}{\Theta_{r1}\Theta_{r2}} \quad (6.3)$$

where  $\Theta_{r1}$  and  $\Theta_{r2}$  are the half-power beam widths in two perpendicular planes in radians.

Figures 6.3 and 6.4 show the radiation pattern of a  $\lambda/2$  dipole antenna above a perfectly conducting ground plane at  $\Phi = 0^\circ$  and  $90^\circ$  obtained from NEC2.

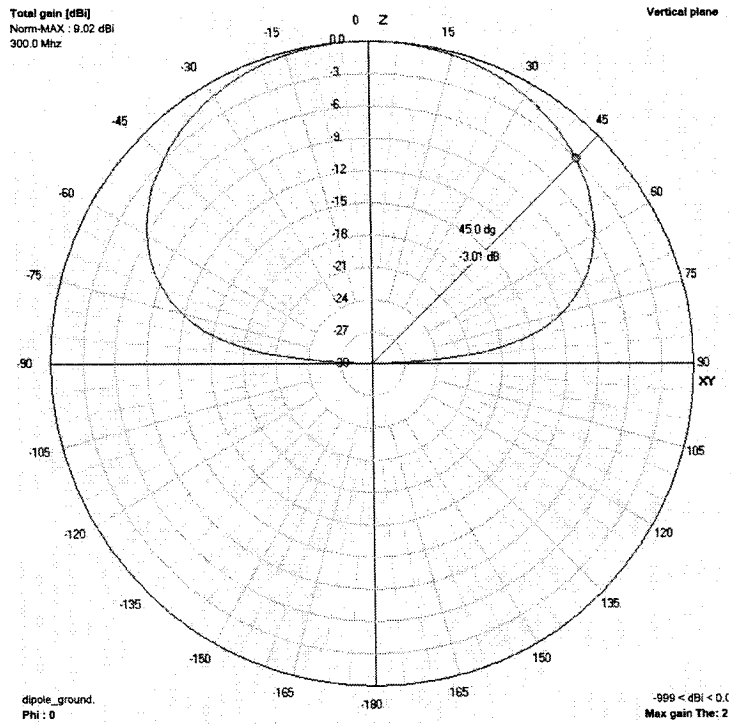


**Figure 6.3:** Radiation pattern at  $\Phi = 0^\circ$

Figure 6.3 shows the radiation pattern of a  $\lambda/2$  dipole antenna, placed along the y axis in the xy plane, above a perfectly conducting ground plane at  $\Phi = 0^\circ$ . The half-power beam width is  $90^\circ$ .



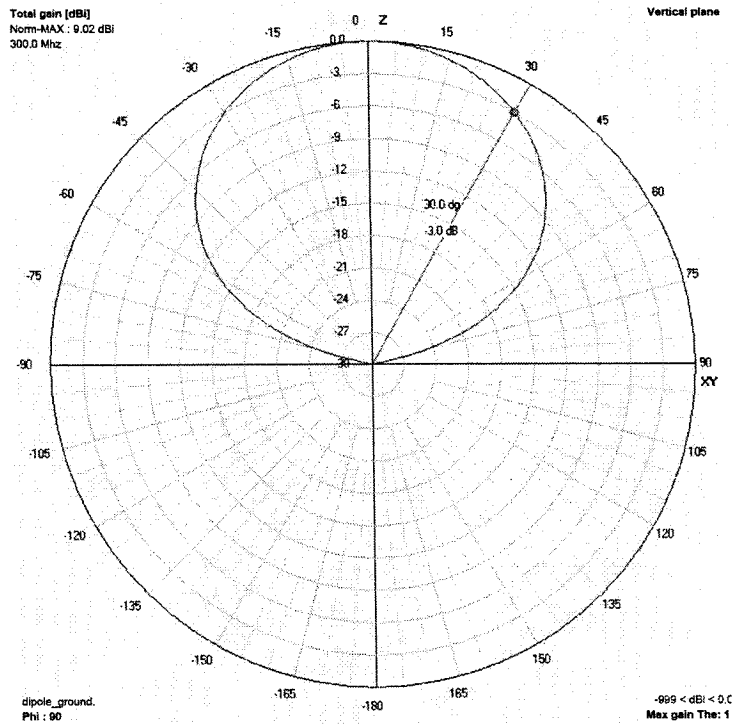


**Figure 6.4:** Radiation pattern at  $\Phi = 90^\circ$

Figure 6.4 shows the radiation pattern of a  $\lambda/2$  dipole antenna, placed along the y axis in the xy plane, above a perfectly conducting ground plane at  $\Phi = 90^\circ$ . The half-power beam width is  $60^\circ$ .

Hence,

$$\theta_{r1} = 90^\circ \text{ and } \theta_{r2} = 60^\circ, \text{ and}$$

$$D_o = 7.639 = 8.83 \text{ dB}$$

For omni-directional patterns, the maximum directivity  $D_o$  is expressed by [25]:

$$D_o = -172.4 + 191 \sqrt{0.818 + \frac{1}{HPBW(\text{degrees})}} \quad (6.4)$$

Figure 6.5 shows the radiation pattern of a  $\lambda/2$  dipole antenna placed along the y axis in the xy plane in free space.

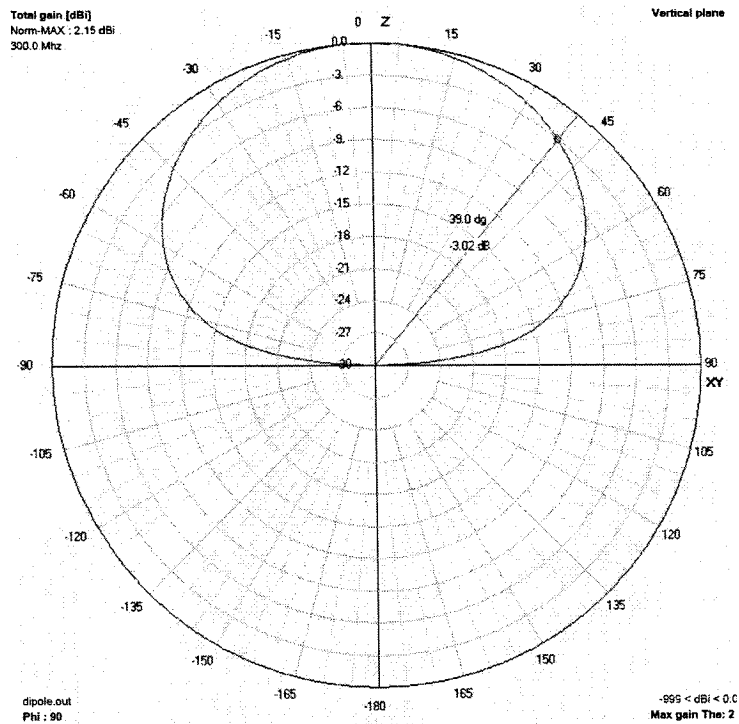


Figure 6.5: Radiation pattern at  $\Phi = 90^\circ$

HPBW =  $76^\circ$ , hence,  $D_o = 1.73 = 2.38$  dB.

There is a gain of about 6.45 dB when using a  $\lambda/2$  dipole antenna above ground plane. Therefore, the MSE performance of the DoA estimation system is expected to be enhanced considerably.

### 6.3 Simulations Results

To this end, the integrated NEC2-Matlab system is ready to be deployed with the MLM for DoA estimation. Several cases are going to be compared and discussed

to illustrate the performance enhancement achieved by methods of element selection and changing the spacing between the elements.

Figure 6.6 shows a comparison in performance in terms of MSE between a 5-element linear  $\lambda/2$  dipole array and a 5-element linear  $\lambda/2$  dipole array above perfectly conducting ground plane. The scan range is defined from -10 to 10 degrees in a step of 5 degrees to create the look up table for the MLM. The incident wave is at 5 degrees which is one of the angles the system has been trained on.

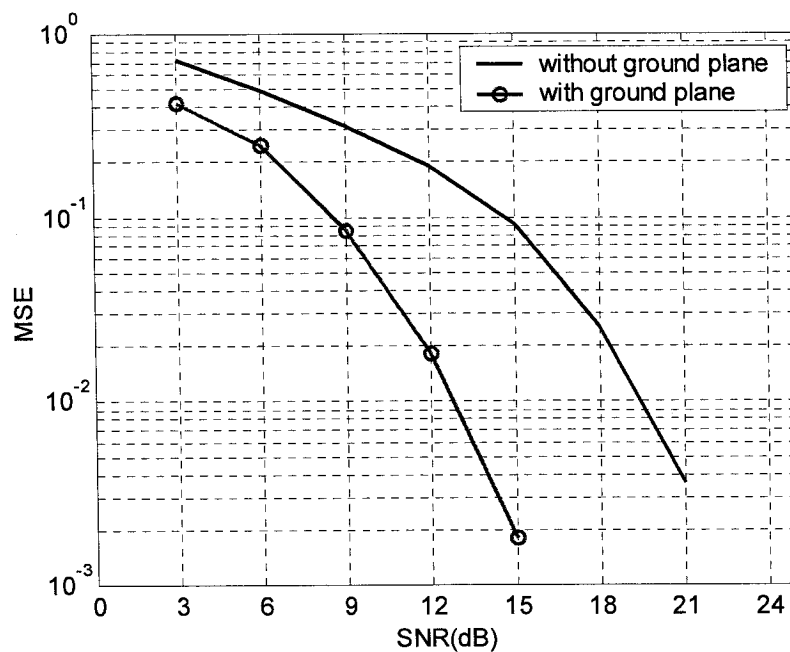


**Figure 6.6:** Comparison in terms of MSE between a 5-element dipole linear array in free space and a 5-element dipole linear array above perfectly conducting ground plane

The utilization of the proposed elements,  $\lambda/2$  dipole antennas above perfectly conducting ground plane, enhanced the performance considerably. At low SNR, there is an enhancement of about 4 dB and increases as SNR to reach about 7 dB.

A logical next step would be to reduce the step size used to create the look up table in order to see its effect on the performance of the DoA system. The new step size used is  $2^\circ$ .

Figure 6.7 shows a comparison in performance in terms of MSE between a 5-element linear  $\lambda/2$  dipole array and a 5-element linear  $\lambda/2$  dipole array above perfectly conducting ground plane. The scan range is defined from -10 to 10 degrees in a step of 2 degrees to create the look up table for the MLM. The incident wave is at 6 degrees which is one of the angles the system has been trained on.

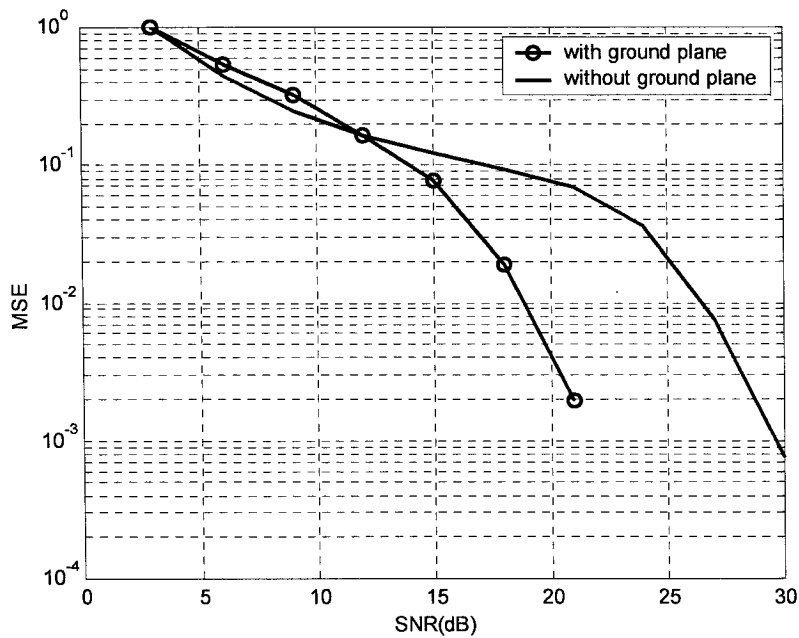


**Figure 6.7:** Comparison in terms of MSE between a 5-element dipole linear array in free space and a 5-element dipole linear array above perfectly conducting ground plane

Reducing the step size resulted in enhancing the performance at SNR higher than 12 dB. The  $\lambda/2$  dipole linear array in free space produced a poor performance when the step size was reduced at SNR higher than 12 dB.

Another approach that was suggested in chapter 3 is to change the spacing between the elements subject to the constraint that the spacing can not exceed a certain value in order to avoid creating grating lobes. This constraint suggests that for a scan range from -10 to 10 degrees, the spacing should not exceed  $0.503 \lambda$ . However, this is valid if the array antenna is in the transmit mode. If we consider the array antenna to be in the receive mode, and one snap shot is only taken to sample the incident wave in order to determine the DoA, then increasing the spacing more than  $0.503 \lambda$  will not affect the performance of the DoA estimation system. It is important to emphasize that this is only valid if we are using one snap shot to sample the incident wave and determine the DoA. If more than one snap shot is used, further investigation should be conducted about the effect of changing the spacing between the elements in the array structure.

Figure 6.8 shows a comparison in performance in terms of MSE between a 5-element linear  $\lambda/2$  dipole array with  $0.5 \lambda$  spacing between the elements and a 5-element linear  $\lambda/2$  dipole array with  $0.6 \lambda$  spacing between the elements. The scan range is defined from -10 to 10 degrees in a step of 5 degrees to create the look up table for the MLM. The incident wave is at 5 degrees which is one of the angles the system has been trained on.

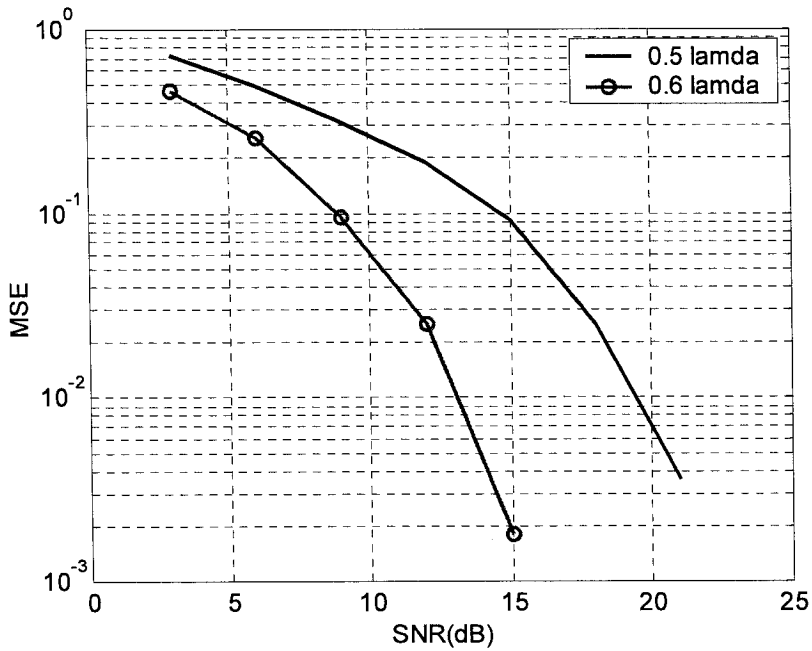


**Figure 6.8:** Comparison in terms of MSE between a 5-element dipole linear array in free space with 0.5 Lambda and 0.6 lambda spacing between the elements

Increasing the spacing between the elements resulted in an enhancement in the MSE performance by almost 4 dB at low SNR up to almost 7 dB at high SNR.

Figure 6.9 shows a comparison in performance in terms of MSE between a 5-element linear  $\lambda/2$  dipole array above perfectly conducting ground plane with  $0.5 \lambda$  spacing between the elements and a 5-element linear  $\lambda/2$  dipole array above perfectly conducting ground plane with  $0.6 \lambda$  spacing between the elements. The scan range is defined from -10 to 10 degrees in a step of 5 degrees to create the look up table for the MLM. The incident wave is at 5 degrees which is one of the angles the system has been trained on.

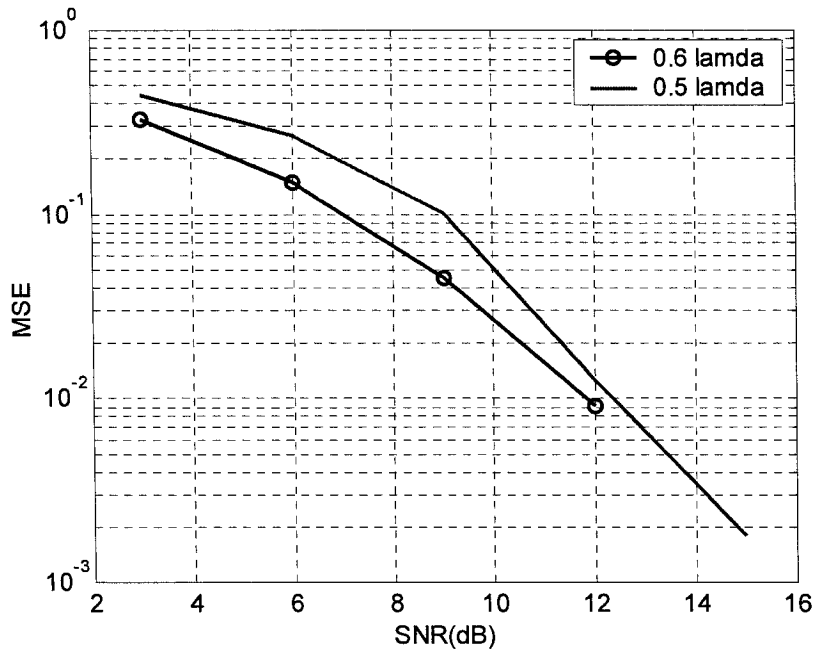


**Figure 6.9:** Comparison in terms of MSE between a 5-element dipole linear array above perfectly conducting ground plane with 0.5 Lambda and 0.6 lambda spacing between the elements

The performance was enhanced in the case of a 5-element linear  $\lambda/2$  dipole array above perfectly conducting ground plane when the spacing between the elements was increased similar to the case of the 5-element linear  $\lambda/2$  dipole array in free space. The amount of enhancement is less but the MSE drops to zero at a lower SNR. In the case of  $0.5 \lambda$ , the MSE drops to zero at SNR = 15 dB, whereas, in the case of  $0.6 \lambda$ , the MSE drops to zero at SNR = 12 dB.

## 6.4 Summary

The results shown in figure 6.6 clearly show that there is a good enhancement in performance. At low SNR, there is a gain of about 4 dB and as SNR increases, the gain increases to reach about 7 dB.

The resolution in the lookup table was changes to  $2^\circ$  instead of  $5^\circ$ . Figure 6.7 shows that the performance of the array without ground plane is poor compared to the array with ground plane at SNR higher than 12 dB. From this, it can be concluded that more directive elements perform better in determining the DoA when the incident signals are close to each other—i.e. 2 degrees apart. The use of more directive elements would enhance the performance as shown in the same figure. For SNR larger than 23 dB, the error drops to zero for 5 element linear dipole array above perfectly conducting ground plane.

Figure 6.8 shows how the performance is affected by changing the spacing between the elements to 0.6 lambda instead of 0.5 lambda. An enhancement in performance, almost equivalent to adding a perfectly conducting ground plane, was achieved. Figure 6.9 shows the same scenario but for an array above perfectly conducting ground plane.

Increasing the spacing between the elements would results in sampling the incident plane wave at locations that are further apart. Therefore, the phase difference between the sampled points would increase and that makes the sampled data less vulnerable to the noise effect.



# Chapter 7

## Conclusion

### 7.1 Summary

The work done in this thesis was performed by first understanding the concept of DoA estimation and realizing its importance and applications. Second, DoA estimation techniques, which vary in principle and applications, were reviewed in order to find the most suitable technique to use in this thesis. The objective was to find a DoA technique that is simple to construct in order to illustrate the effect of mutual coupling and array antenna element selection on the DoA estimation process. It also has to be a technique from which the obtained results could be generalized to more cases rather than one or two cases. The MLM was found to be the DoA technique that mostly suits this objective. Third, the MLM was implemented using both, omni-directional elements and point sources as the array antenna elements. Fourth, NEC2 was introduced and its principal of operation was explained as it is based on finding a numerical solution of integral equations for the induced currents on a structure using the Method of Moments. Also mutual coupling between the array elements was introduced as it affects the overall performance of the array structure in DoA estimation. Simple illustrative experiments of the effect of mutual coupling were presented. Fifth, a NEC2-Matlab interface was implemented in a way such that Matlab takes control over the DoA estimation process and produce MSE graphs for different scenarios. Finally, the NEC2-Matlab integrated system was utilized to obtain MSE results for DoA using the MLM and  $\lambda/2$  dipole antennas as the array elements

and then these results were compared to a set of results obtained by changing the array elements to more directive elements which are  $\lambda/2$  dipole antennas above perfectly conducting ground plane. This change of elements in the array structure produced a significant enhancement in the DoA performance. This implies that there should exist an element selection criterion that provides the optimum array element type for each DoA application. More directive elements provided better MSE performance since one of the major effects on mutual coupling between the array elements in the array environment is the radiation pattern of the elements selected. Another approach that was also tested was changing the spacing between the array elements. This approach, under certain conditions, also showed a significant enhancement in the DoA estimation performance.

The NEC2-Matlab integrated system provided a more realistic environment to assess the performance of the DoA estimation technique. It provided an advantage over the current DoA estimation results available in the literature since there were no assumptions that the elements are completely isolated from each other or that omnidirectional elements are the only choice for the array structure.

The NEC2-Matlab integrated system has the potential of operating in an actual DoA estimation application such as a radar system. This could be easily performed by defining a set of angles from which the incident plane wave is expected to arrive and utilizing the Data Acquisition Toolbox available in Matlab by connecting the array antenna to a pc with NEC2-Matlab integrated system loaded on it.

A limitation that was faced in this thesis was that NEC2 limited the choice of elements for the array. More directive elements such as micro-strip patches are expected to provide better MSE performance. Such elements could be constructed

using other softwares such as HFSS; however, it was impossible to integrate HFSS with Matlab due to its graphical user interface operating nature.

## **7.2 Concluding Remarks**

The integration of NEC2 and Matlab created an environment similar to the environment an actual array would operate in. This was achieved by accounting for mutual coupling between the array elements which showed to have a significant effect on the array performance in the transmit and receive modes as well as on the MSE performance. Changing the elements type to more directive elements enhanced the MSE performance in all cases. The 5-element linear  $\lambda/2$  dipole array possessed a poor performance when the incident signals were  $2^\circ$  apart whereas the proposed elements—i.e.  $\lambda/2$  dipole antennas above perfectly conducting ground plane showed great potential in determining the DoA. This indicated that the use of more directive elements in the array structure would enhance the performance of the DoA estimation when the incident waves are closely spaced, in this case  $2^\circ$  apart. This proves that optimum selection criteria should be adopted in conjunction with the DoA estimation algorithm in order to minimize the estimation MSE.

Another important observation was that the MSE performance was enhanced when the spacing between the array elements was changed. The degree of enhancement was higher for the 5-element linear dipole array in free space than the 5-element linear dipole array above perfectly conducting ground plane. A point that is worth mentioning is that changing the spacing between the elements is subject to a certain criteria in which avoiding creating grating lobes should be considered.

Although the array under consideration is in the receive mode, as soon as its elements are excited with the plane wave incident upon them, they will start radiating. If the spacing between the elements is not calculated in such a way to avoid creating grating lobes and to minimize mutual coupling, then the resulting radiation pattern's maxima could be misplaced from the DoA of the incident plane wave. Therefore, the proposed spacing for the range of -10 to 10 degrees was valid only if one snapshot was taken to sample the incident wave.

### **7.3 *Future Work***

The scope of this thesis could be extended to cover many topics that could be of interest for further research and investigation. One possible choice would be investigating how choosing more directive elements affects the performance. This thesis presented a  $\lambda/2$  dipole antenna above perfectly conducting ground plane as the more directive element than a conventional  $\lambda/2$  dipole antenna in free space. The results were very promising and encouraging to pursue further research on this path.

Another option would be utilizing a planar array instead of a linear array in conjunction with the optimum element type selection criterion. Further more, a DoA estimation algorithm, other than MLM, could be investigated and its performance could be assessed based on element type selection. Since the number of elements in real application is limited, then the optimality situation of the DoA estimation algorithm could be considered in more details and an algorithm such as MUSIC could be adopted. Finally, considering more than one plane wave incident at a time is another option. NEC2 allows the user to create one incident plane wave at a time, therefore, the user should create multiple signals incident from different directions

and add the phase manually, either constructively or destructively, depending on the situation in hand. The phase addition process could be done using Matlab to make it more time and effort efficient.

## References

- [1] Stoica P. and Sharman K. C., "Maximum Likelihood Methods for Direction of Arrival Estimation," *IEEE Trans. Acoust., Speech, Signal Processing*, vol. 38. No. 7, pp. 1132-1143, July 1990.
- [2] Ziskind I. and Wax M., "Maximum Likelihood Localization of Multiple Sources by Alternating Projection," *IEEE Trans. Acoust., Speech, Signal Processing*, vol. 36. No. 10, pp. 1553-1560, October 1988.
- [3] Stoica P. and Nehorai A., "MUSIC, Maximum Likelihood, and Cramer-Rao Bound," *IEEE Trans. Acoust., Speech, Signal Processing*, vol. 37. No. 5, pp. 720-741, May 1989.
- [4] Stoica P. and Nehorai A., "MUSIC, Maximum Likelihood, and Cramer-Rao Bound: Further Results and Comparisons," *IEEE Trans. Acoust., Speech, Signal Processing*, vol. 38. No. 12, pp. 2140-2150, December 1990.
- [5] Lal C. Godara "Application of Antenna Arrays to Mobile Communications, Part II: Beam-Forming and Direction-of-Arrival Considerations." *IEEE Proceedings*, Vol. 85, No. 8, August 1997.
- [6] James W. Dietrich, "A Novel Nec2/Matlab Interface Applied To A Study of Adaptive Antenna Array Signal Processing," M.Sc Thesis, Department of Electrical and Computer Engineering, University of Manitoba, March 2004.
- [7] J. Capon, "High-resolution frequency-wave number spectrum analysis," *Proc. IEEE*, vol. 57, pp. 1408-1418, 1969.
- [8] D. H. Johnson, "The application of spectral estimation methods to bearing estimation problems," *Proc. IEEE*, vol. 70, pp. 1018-1028, 1982.

- [9] Q. T. Zhang, "A statistical resolution theory of the beamformer-based spatial spectrum for determining the directions of signals in white noise," *IEEE Trans. Signal Processing*, vol. 43, pp. 1867-1873, 1995.
- [10] M. I. Miller and D. R. Fuhrmann, "Maximum likelihood narrow-band direction finding and the EM algorithm," *IEEE Trans. Acoust. Speech, Signal Processing*, vol. 38, pp. 1560-1577, 1990.
- [11] S. B. Kesler, S. Boodaghians, and J. Kesler, "Resolving uncorrelated and correlated sources by linear prediction," *IEEE Trans. Antennas Propagat.*, vol. AP-33, pp. 1221-1227, 1985.
- [12] T. Thorvaldsen, "Maximum entropy spectral analysis in antenna spatial filtering," *IEEE Trans. Antennas Propagat.*, vol. AP-28, no. 99, pp. 556-562, 1980.
- [13] S. W. Lang and J. H. McClellan, "Spectral estimation for sensor arrays," *IEEE Trans. Acoust., Speech, Signal Processing*, vol. ASSP-31, pp. 349-358, 1983.
- [14] R. O. Schmidt, "Multiple emitter location and signal parameter estimation," *IEEE Trans. Antennas Propagat.*, vol. AP-34, pp. 276-280, 1986.
- [15] R. D. DeGroat, E. M. Dowling, and D. A. Linebarger, "The constrained MUSIC problem," *IEEE Trans. Signal Processing*, vol. 41, pp. 1445-1449, 1993.
- [16] B. Friedlander, "A sensitivity analysis of MUSIC algorithm," *IEEE Trans. Acoust., Speech, Signal Processing*, vol. ASSP-38, pp. 1740-1751, 1990.
- [17] M. D. Zoltowski, G. M. Kautz, and S. D. Silverstein, "Beamspace root-MUSIC," *IEEE Trans. Signal Processing*, vol. 41, pp. 344-364, 1993.

- [18] R. Kumaresan and D. W. Tufts, "Estimation the angles of arrival of multiple plane waves," *IEEE Trans. Aerosp. Elect. Systems*, Vol. AES-19, pp. 134-139, 1983.
- [19] S. S. Reddi, "Multiple source location—A digital approach," *IEEE Trans. Aerosp. Electron. Syst.*, vol. AES-15, pp. 95-105, 1979.
- [20] K. M. Buckley and X. L. Xu, "Spatial spectrum estimation in a location sector," *IEEE Trans. Acoust., Speech, Signal Processing*, vol. ASSP-38, pp. 1842-1852, 1990.
- [21] R. Roy and T. Kailath, "ESPRIT—Estimation of signal parameters via rotational invariance techniques," *IEEE Trans. Acoust., Speech, Signal Processing*, vol. ASSP-37, pp. 984-995, 1989.
- [22] M. Viberg and B. Ottersten, "Sensor array processing based on subspace fitting," *IEEE Trans. Signal Processing*, vol. 39, pp. 1110-1121, 1991.
- [23] M. Viberg, B. Ottersten, and T. Kailath, "Detection and estimation in sensor arrays using weighted subspace fitting," *IEEE Trans. Signal Processing*, vol. 39, pp. 2436-2449, 1991.
- [24] G.J. Burke and A.J. Poggio: Numerical Electromagnetic Code: NEC-2 Manual, Lawrence Livermore Laboratory, 1981.
- [25] C. A. Balanis, *Antenna Theory Analysis and Design*, John Wiley and Sons, Inc., New York, 1982.
- [26] The MathWorks, Inc. internet website,  
<http://www.mathworks.com/products/matlab/index.html?ref=pfo>
- [27] Walpole, Mayers, Mayers, Ye, "*Probability and Statistics for Engineers and Scientists*", Seventh Edition, Prentice Hall.



- [28] Burke, G.J. and Poggio, A.J., "Numerical Electromagnetic Code (NEC) - Method of Moments", *NOSC Technical Document 116*, Naval Ocean Systems Center, Jan. 1980.
- [29] J. H. Richmond, "A Wire-Grid Model for Scattering by Conducting Bodies," *IEEE Trans. Antennas Propagat.*, Vol. AP-14, No. 6, pp. 782-786, November 1966.
- [30] C. M. Butler and D. R. Wilton, "Evaluation of Potential Integral at Singularity of Exact Kernel in Thin-Wire Calculations," *IEEE Trans. Antennas Propagat.*, Vol. AP-23, No. 2, pp. 293-295, March 1975.
- [31] D. R. Wilton and C. M. Butler, "Efficient Numerical Techniques for Solving Pocklington's Equation and their Relationships to Other Methods," *IEEE Trans. Antennas Propagat.*, Vol. AP-24, No. 1, pp. 83-86, January 1976.
- [32] R. F. Harrington, *Field Computation by Moment Methods*, Macmillan, New York, 1968.
- [33] W. L. Stutzman and G. A. Thiele, *Antenna Theory and Design*, John Wiley and Sons, Inc., New York, 1981.
- [34] John L. Allen, "Gain and impedance Variation in Scanned Dipole Arrays," *IRE Transactions on Antennas and Propagation*, pp. 566-572, September 1962.
- [35] L. A. Kurtz, *et al.*, "Mutual-coupling effects in scanning dipole arrays," *IRA Trans. on Antennas and Propagation*. Vol. AP-9 pp. 433-443; September, 1961.
- [36] D. M. Pozar, *Microwave Engineering*, Second Edition, John Wiley and Sons, Inc., New York, 1998.